JNCC Report

No: 571

Geological investigation of pockmarks in the Braemar Pockmarks SCI and surrounding area

Gafeira, J. & Long, D.

August 2015

0963 8091

For further information please contact:

Joint Nature Conservation Committee
Monkstone House
City Road
Peterborough PE1 1JY
www.jncc.defra.gov.uk

This report should be cited as:

Gafeira, J. & Long, D. 2015. Geological investigation of pockmarks in the Braemar Pockmarks and surrounding area. *JNCC Report No 571*. JNCC Peterborough.

Foreword

This report is the product of a desk study by the British Geological Survey (BGS) for the Joint Nature Conservation Committee (JNCC). The scope of the desk study included a comparison of the JNCC 2012 multibeam/side-scan dataset from the Scanner and Braemar pockmarks areas in the Northern North Sea with similar historic datasets noting morphological change. Also within scope were a record of observations of gas seepage and Methane-Derived Authigenic Carbonate (MDAC), an examination of sedimentation rates and evidence of anthropogenic causes of sedimentation. The aims and objectives are given in the Scope of work (Appendix 1).

This report contains the analysis of the Braemar Pockmarks SCI area. The results from the Scanner Pockmark SCI are given in a separate report.

The Braemar Pockmarks site proposal was submitted to the European Commission on 31st August 2008 for the following interest feature under the EC Habitats Directive: 1180 Submarine structures made by leaking gases. Following submission, it was accepted as a Site of Community Importance (SCI). The Braemar Pockmarks SCI area is located in UKCS blocks 9/28 and 16/3.

Prior to publication this report was subject to JNCC's Evidence Quality Assurance (EQA) process and was peer reviewed by Dr Alan Judd and Peter Croker. The JNCC EQA policy can be found on the JNCC website. http://jncc.defra.gov.uk/default.aspx?page=6675

Acknowledgements

Taqa Bratani Ltd of the Abu Dhabi National Energy Company is thanked for giving permission to use data originally collected for BP from the Harding Development relating to the Harding to East Brae pipeline route survey.

We thank Dr Alan Judd, Peter Croker and JNCC for their comments on an earlier version of this report.

British Geological Survey
NATURAL ENVIRONMENT RESEARCH COUNCIL

Contents

FIGURES

TABLES

Summary

This report describes the findings of a desk study carried out by British Geological Survey (BGS) for the Joint Nature Conservation Committee (JNCC) covering the Braemar Pockmarks SCI area. The Braemar Pockmarks SCI is located in the UK Northern North Sea in the vicinity of the Braemar field (UKCS Block 16/3). This site was submitted to the European Commission on 31st August 2008, under the EC Habitats Directive: *1180 Submarine structure made by leaking gases*, and was approved as a Site of Community Importance (SCI) by the European Commission.

This study's focus is on the pockmarks found in and around the Braemar Pockmarks SCI area, and looks at specific factors that influence the formation and exposure of carbonate structures within the pockmarks. The new data collected on a JNCC research cruise at the end of 2012, cruise CEND19x/12, in partnership with the Centre for Environment, Fisheries & Aquaculture Science (CEFAS) provided the main dataset for this study. The multibeam dataset collected was used to semi-automatically map and characterise the morphology of the pockmarks. The information extracted from the mapped pockmarks was then compared to the information extracted from previous surveys collected for BP. Backscatter data and side-scan sonar data was used to characterise the nature of the seafloor, in particular the presence of Methane-Derived Authigenic Carbonate (MDAC).

This report's first section introduces the project area. Details of the datasets used are given in section two. JNCC supplied data collected on its 2012 cruise CEND19x/12. BGS's own data was limited to a few seismic profiles across the SCI and some samples located just beyond its boundaries. The third dataset had been collected for BP in 2006 but, following Taqa Britani Ltd acquiring BP's Harding Field interests, permission was sought from the latter to use the dataset to provide a temporal comparison with that collected for JNCC. Section three describes the method of how the multibeam datasets were analysed in a semi-automatic way to remove interpreter bias. It reviews differences identified, assessing whether they reflect true changes or are artefacts of data acquisition. The fourth section reviews evidence, direct and indirect, for gas seepage, and identifies where these have been recorded in the various datasets in the area of the Braemar Pockmarks SCI. Pockmark formation and change have to be considered in the context of natural geological processes and anthropogenic activities; these are covered in sectionss five and six respectively. The results of this study are discussed in section seven together with thoughts on taking the study further in future surveys. The analysis of the multibeam surveys shows 49 pockmarks more than 20 m diameter, with the largest being 200 m in diameter. These are almost equally split in distribution between inside and outside the Braemar Pockmarks SCI area. Some of which show change in their morphology reflecting slope failure, supporting the interpretation that these pockmarks are sites of active processes. There is strong evidence of active gas seepage, in the form of multiple indicators suggesting the presence of MDAC and bacterial mats on the seabed, and gas bubbles in the water column.

The results indicate that the Braemar Pockmarks SCI area is a location of active gas seepage, which should be monitored regularly to check if the features of interest are being compromised by natural or anthropogenic processes and to assess if the limits of the protected area are the most appropriate.

1. Introduction

The Braemar Pockmarks SCI is situated in the Northern North Sea and its boundaries straddle across UK licence blocks 16/3 and 9/28 (Figure 1), approximately 240 km east of the Orkney Islands (site centre at 58º59'12''N, 1º28'34''E). The water depth in the Braemar Pockmarks SCI ranges from 121 m on the northern edge to 124 m on the southern edge of the SCI area.

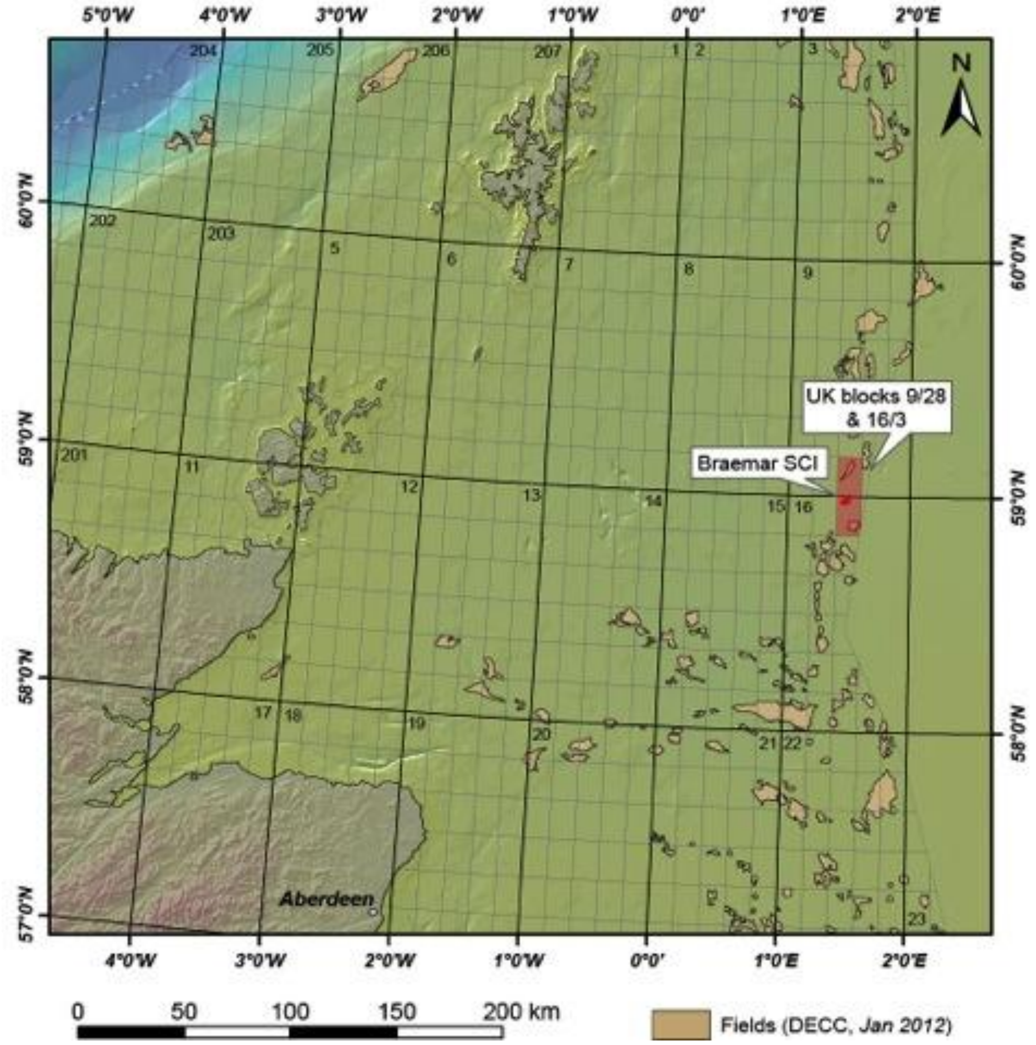

Figure 1. Location of the offshore Braemar Pockmarks Site of Community Importance (SCI) and the oil fields within the Northern North Sea.

The Braemar Pockmarks SCI is situated just to the north of the Witch Ground Basin, a topographical basin 80 km wide, reaching 150 m water depth (Figure 2). This is an extensive area of pockmarks that have been studied since the early 1970s (Judd and Hovland, 2007). Pockmarks are shallow seabed depressions (~2 m depth), several tens of meters across (typically ~70 m), which were probably formed by the venting of biogenic/petrogenic liquids and gases into the water column. Most of the pockmarks in the Witch Ground Basin occur in very soft muds. The pockmarks of the Braemar SCI occur in firmer, slightly coarser sediments. Some contain blocks similar to pavement slabs and smaller fragments of sediment cemented by Methane-Derived Authigenic Carbonate (MDAC). These carbonates are formed by precipitation during the anaerobic oxidation of methane gas within sediments close to the seafloor (Boetius *et al.*, 2000), and when exposed provide a habitat for marine fauna usually associated with hard substrates (Dando *et al.*, 1991). There are also present specific chemosynthetic organisms that feed off both methane and its by-product, hydrogen sulphide (Judd, 2001). The larger blocks of carbonate also provide shelter for fish species such as wolf-fish and cod (JNCC, 2012).

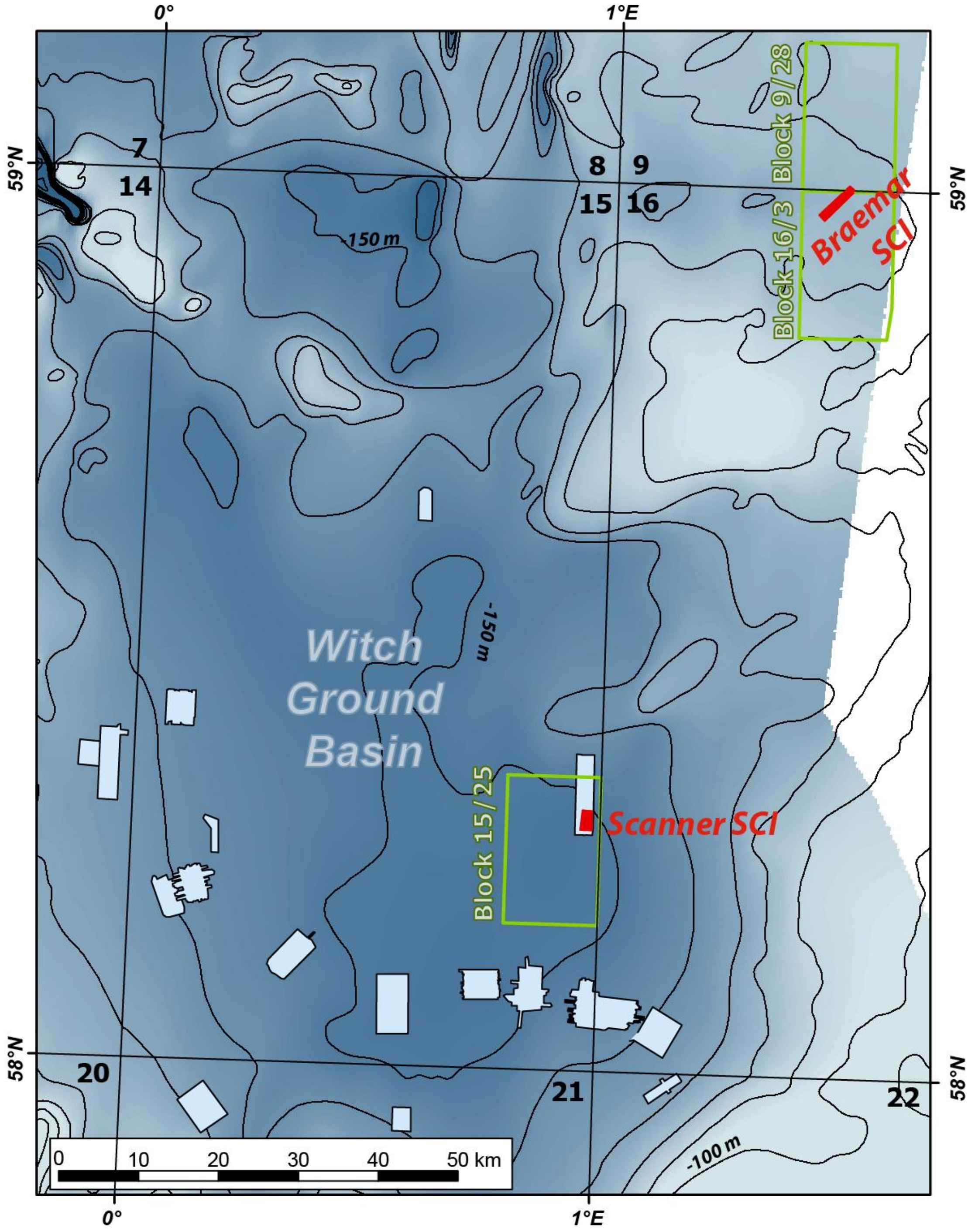

Figure 2. Location of Braemar and Scanner SCIs

Note the location of Braemar SCI away from the main seabed depression of the Witch Ground Basin. The pale blue blocks in the southern part of the Witch Ground Basin are areas of detailed pockmark studies using multibeam data (Gafeira *et al*., 2012).

2. Data sources

2.1. Data supplied by JNCC

JNCC supplied BGS with digital copies of seabed data collected on a JNCC research cruise at the end of 2012 (cruise CEND19x/12) run in partnership with the Centre for Environment, Fisheries & Aquaculture Science (CEFAS). The survey took place between the 17th November and the 1st December 2012 on-board the *CEFAS Endeavour*. These data were transferred via an external hard disk received by post on 17th June 2013. The dataset received is summarized in Table 1. JNCC also supplied, via Dropbox, the survey report for the cruise CEND19x/12.

Table 1. List of data collected from the Braemar Pockmarks SCI study area during the CEND19x/12 cruise and provided to BGS

Data provided
Multibeam Echosounder *(Simrad EM2040)*
Nearly full MBES data coverage comprising: • 32 files of raw data, • processed data for both the backscatter and the bathymetric datasets, and • CARIS project with the multibeam data. (a small area was not covered due to obstruction caused by a well head)
Backscatter
Several geotiffs and raster files were provided including: • IMAGINE image file *BRMR_FP_0d3.img*, mosaic at a 0.3 m resolution,
Bathymetry
Several geotiffs and raster files, including: • IMAGINE image file *BRMR_18032013_MBFP_2d0_UTM31.img*. This raster has a cell size of approximately 2 m.
Side-Scan Sonar (*Edgetech 4200 MP*)
Both raw and processed data providing partial coverage of Braemar SCI: • *Low Frequency (300 kHz):* Partial coverage: a mosaic of seven lines and 12 individual section files, and • *High Frequency (600 kHz):* Limited coverage: nine lines split into 12 sections files.
Groundtruthing
Drop Camera
A total of 77 video clips and 600 stills obtained during 22 drop camera transects plus: • two Excel files • CEFAS' *MPA Video Analysis Report* summarising the analysis of the data • shapefile '*video_tow.shp'* showing the route of the video tows • additional shapefiles showing the location of samples where MDAC was observed
Grab
0.1 m^2 grab samples were subsampled for Particle Size Analysis (PSA), the remaining material was washed over 5 mm and 1 mm sieves to retain benthic fauna. • Particle Size Analyses - also provided as ArcGIS' point shapefile (*Braemar_PSA.shp*) • photos of the grabs on 5 mm sieves • 3 Microsoft Excel files summarising sample details • benthic fauna data matrix • additional shapefile showing the location of samples where MDAC was found.

Prior to recommending Braemar Pockmarks as a proposed Special Area of Conservation (SAC), JNCC commissioned a report from Hartley Anderson Ltd on pockmarks in Block 16/3 (Hartley, 2005). A copy of this report had already been supplied to BGS by Fionnuala McBreen (JNCC, on 18/11/2011).

During that study 53 pockmarks were identified in area of 16 km^2 centred on 1° 28' 51.1697"E, 58° 58' 54.3305"N. There is an overlap with the 2012 JNCC multibeam dataset of more than 50%. Hartley’s dataset comprised: a 1995 rig site survey that included side-scan sonar, a subsequent 2001 pipeline survey, and an ROV survey from 2003. The last survey provided photographic and video evidence of the seabed features mapped by the side-scan sonar interpretation (Hartley, 2005).

2.2. BGS-acquired data

As well as the published maps [Bressay Bank, Sheet 59° N-00°, 1:250,000 Series, Seabed Sediments (published 1987) and Quaternary Geology (published 1986); Fladen, Sheet 58° N-00°, 1:250,000 Series, Seabed Sediments (published 1986) and Quaternary Geology (published 1988)] and the regional report (Johnson *et al*., 1993), the original sampling records (seabed grab, vibrocore) and geophysical data (primarily deep tow boomer, sparker and side-scan sonar) provide information on the shallow geological and seabed conditions (for locations see Table 2, Figure 3 and Appendix 5). These data were primarily collected in the 1970s and 1980s as part of the regional mapping programme on behalf of the Department of Energy, later Department of Trade and Industry. It has been supplemented by additional data from commercial and governmental sources. Details from the Sea Bed Sediments maps are available digitally within the DigBath250 and DigSBS250 products and have been used in this study to provide information at a regional level.

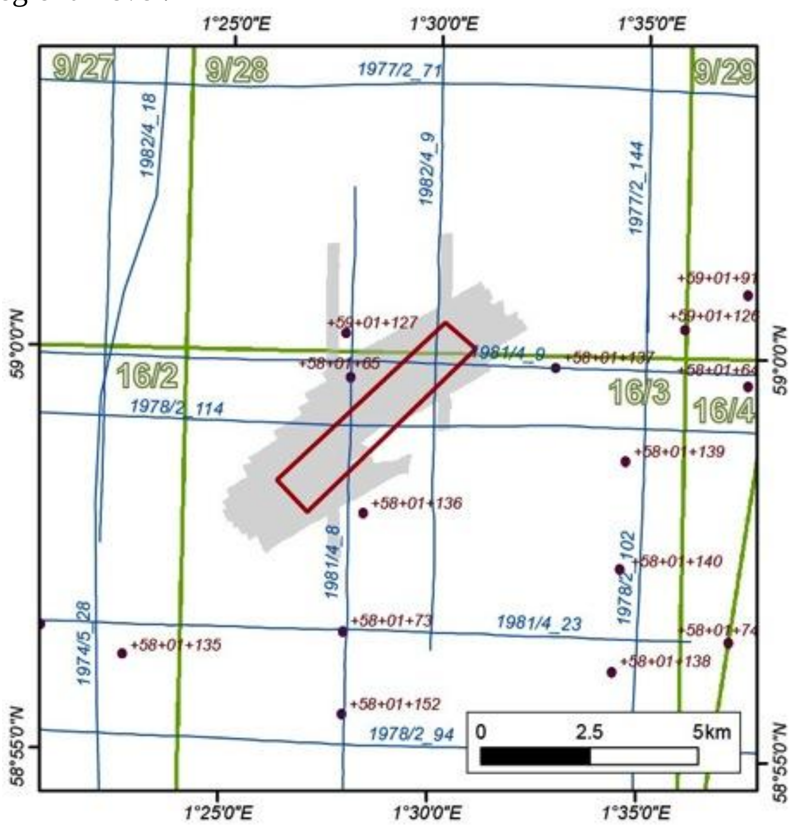

Figure 3. BGS data around Braemar Pockmarks SCI.

The grey area shows the area covered by the JNCC multibeam dataset. Blue lines and annotations indicate BGS geophysical survey lines. Red crosses and annotation indicate the locations of BGS seabed samples. Green lines and numbers indicate block boundaries/numbers (and the UK/Norway median line).

There is a suite of shallow seismic lines across the Braemar Pockmarks SCI area (Figure 3). Some of the BGS air-gun, sparker, boomer, and side-scan survey records and site investigation report data are only available in hardcopy format. None of the BGS seabed samples are located within the Braemar Pockmarks SCI area; however there are 8 samples within less than 5 kilometres. Details of these samples are given in Table 2 and their locations can be seen in Figure 3.

Table 2. BGS seabed samples within 5 kilometres of the Braemar SCI area.

TD stands for total depth reached in metres.

Sample Station	*Year*	*Water Depth (m)*	*Latitude*	*Longitude*	*TD*	*Description*
+58+01/65	1981	120	58.99523	1.46784	0.96	grey-green muddy slightly sandy foraminifera-rich silt over grey-green silty sand
+58+01/73	1981	139	58.94266	1.46688	1.2	olive silty slightly sandy mud over olive silty sand with H_2S smell
+58+01/136	1982	125	58.96718	1.47415	6.03	olive-green muddy heavily bioturbated sand,few whole shells
+58+01/137	1982	122	58.99812	1.54979	5.93	very muddy olive-green bioturbated and core-disturbed sand
+58+01/139	1982	123	58.97908	1.57867	0.77	olive mud/olive grey muddy sand/dark grey muddy sand
+58+01/152	1982	122	58.92562	1.46725	0.1	olive mud/very fine olive sand
+59+01/126	1983	121	59.0065	1.60133	0.2	olive muddy fine sand moderately well sorted
+59+01/127	1983	125	59.00433	1.46567	0.87	poorly sorted olive muddy sand over grey muddy sand

2.3. Third party data held by the BGS

BGS regularly requests operators to deposit copies of site investigations and other shallow data within its national archives. These data are held as commercial in confidence but are used to update regional maps and interpretation. Prior to the commissioning of this study, BP had deposited reports and the associated xyz data from multibeam surveys conducted by Gardline in 2006 as part of its Harding development.

Gardline, 2006. UKCS 9/23, 9/28 and 16/3, Harding to East Brae pipeline route survey for BP Exploration Operating Company Ltd. May/June 2006. Survey report volume 1 – results. Project Ref. 6704.1

Gardline, 2007. UKCS 9/23, 9/28 and 16/3, Harding to East Brae pipeline route survey for BP Exploration Operating Company Ltd. May/June and September 2006. Survey report volume 1 – results. Project Ref. 6704.1 and 7000

On 1st June 2013 BP sold its interests in the Harding Field to Taqa Bratani Ltd of the Abu Dhabi National Energy Company. So, to ensure full agreement, permission to use these data was sought from the new owners. Permission to use these data in the current study was given by Britta Hallbauer of Taqa Britani Ltd in an e-mail to Dave Long dated 29th August 2013.

2.4. Multibeam surveys

A significant part of this study was based on the interpretation and analysis of the multibeam datasets acquired on a JNCC research cruise, cruise CEND19x/12, in partnership with the Centre for Environment, Fisheries & Aquaculture Science (CEFAS) in 2012, and by Gardline for BP in 2006 (Figure 4). The JNCC dataset was imported into ArcMap as a 2 m cell size grid, whereas the BP dataset was imported as a 5 m cell size grid. The BP dataset was re-projected to match with the JNCC dataset, which uses an UTM 31N projection and WGS 1984 datum.

The BP dataset covers a much wider area than that covered by the JNCC survey or the Braemar Pockmarks SCI area (Figure 4). Pockmarks can be seen in this wider area, most notably in the channel south of Braemar Pockmarks SCI (Figure 4), however this report does not consider pockmarks beyond the limits of the JNCC survey.

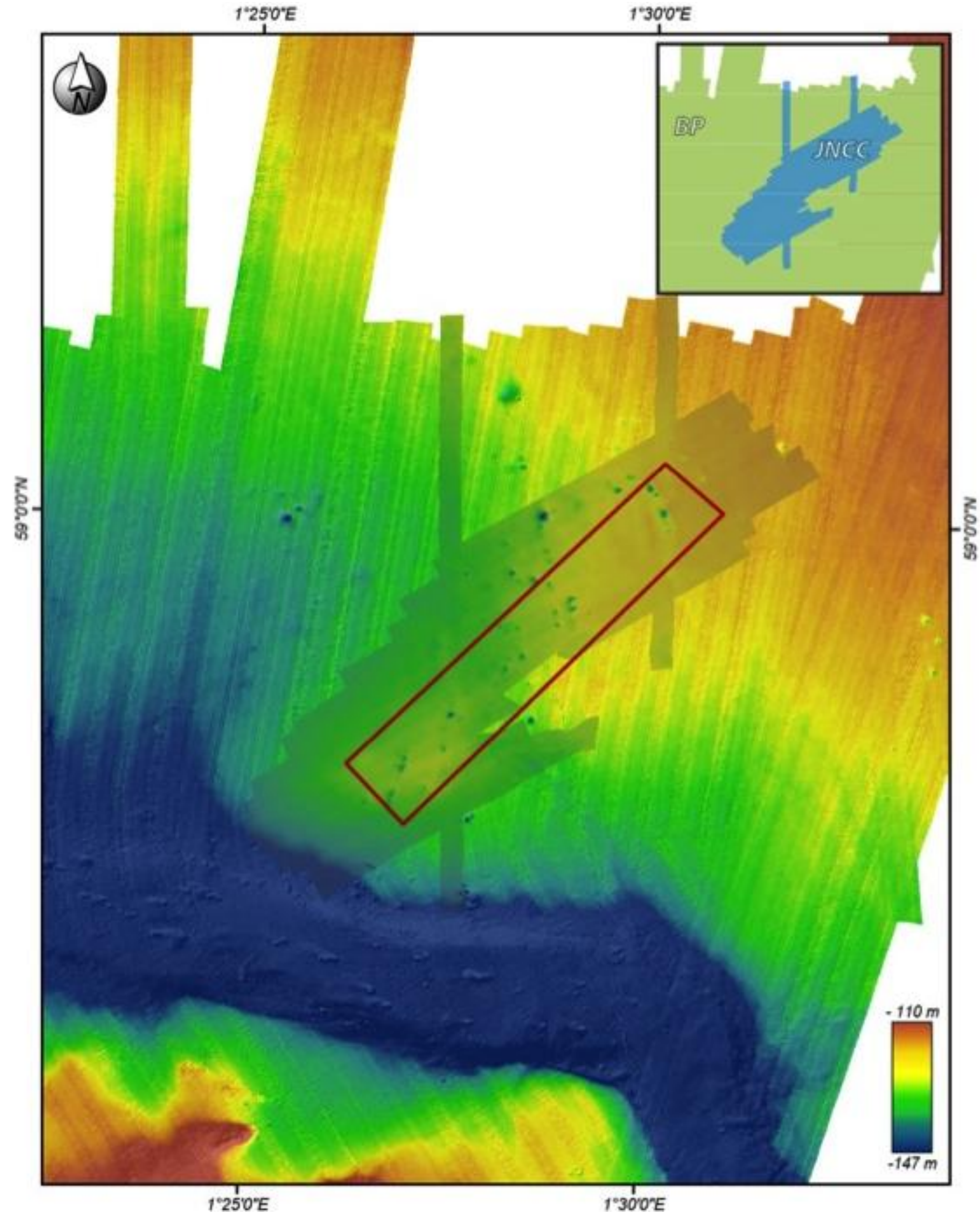

Figure 4. Bathymetric map showing the multibeam data used during this study.

The red outline shows the limits of the Braemar Pockmarks SCI. Note that the BP survey with its much wider regional coverage shows pockmarks beyond the area of the JNCC commissioned survey.

3. Braemar Pockmarks SCI

3.1. Semi-automated mapping

A semi-automated method of mapping and morphometric characterization was used to map the pockmarks within both multibeam surveys used in this study. This semi-automated method allows the systematic application of a sequence of well-defined tools available within the ESRI ArcGIS toolbox (Gafeira *et al.*, 2012). The input dataset required is merely a digital depth model (DDM) that is used to generate three output shapefiles:

1) a polygon shapefile that delineates the pockmarks at seabed,
2) a point shapefile that shows the centroid of the referred polygons,
and
3) a point shapefile that marks the deepest point within each pockmark mapped.

This last shapefile is likely to correspond to the main source point, or vent, of the fluid escape that originated the formation of the pockmark. These output shapefiles include, within their table of attributes, a series of morphometric attributes measured for each mapped pockmark: area (m^2), perimeter (m), area/perimeter ratio, depth (m), maximum water depth, minimum water depth, maximum slope, mean slope, azimuth and major axis length.

This semi-automated method requires the definition, by the user, of three threshold values for the pockmarks: *Minimum Depth*, *Minimum Area* and *Minimum Area/Perimeter Ratio*. The thresholds used for this study were 40 cm, 300 m^2 and 4.5 m respectively. The user must also define a *Buffer Distance,* which will reflect approximately the distance, in plan-view, from the internal contour line delineated, by the automated method, to the actual rim of the pockmarks. The *Buffer Distance* used for this study was 7.5 m.

This method makes it possible to extract morphologic information on a vast number of pockmarks from multiple surveys in a fast, systematic and consistent way. This is a significant improvement to the study of pockmarks, considering that it would be highly unlikely for one or multiple interpreters to maintain the same criteria throughout the laborious process of manually mapping large numbers of pockmarks, therefore compromising validity of statistical comparisons between pockmark populations.

3.2. Pockmarks Morphological Description

Using the method described above, 50 seabed depressions were mapped within the area covered by the JNCC multibeam dataset (Figure 5). It was observed that there are additional depressions of smaller dimensions that were not mapped by the automated method; for example the one located at 1°28'4.44"E, 58°59'2.28"N. These depressions, which are no more than 40 cm deep and generally less than 20 m wide, were not mapped because their dimensions are close to the noise values within the data. Nevertheless, two pockmarks shallower than 40 cm were manually mapped (pockmarks 5 and 7) because their areas are considerably greater than other pockmarks with similar vertical relief.

Based on the detailed observation of the morphology of the mapped depressions, it was concluded that the depression named pockmark 2 is a case of a false-positive, *i.e.* a feature mapped as being a pockmark without actually being one. This apparent pockmark presents a near perfect conical shape and it is believe to result from the drilling of the exploration well 16/03c-12 (plugged and abandoned on 14th December 1990) at this location. All the remaining depressions were considered to correspond reliably to accepted definitions of pockmarks (Judd and Hovland, 2007). Their outlines and details are presented in Figure 5 and Table 3.

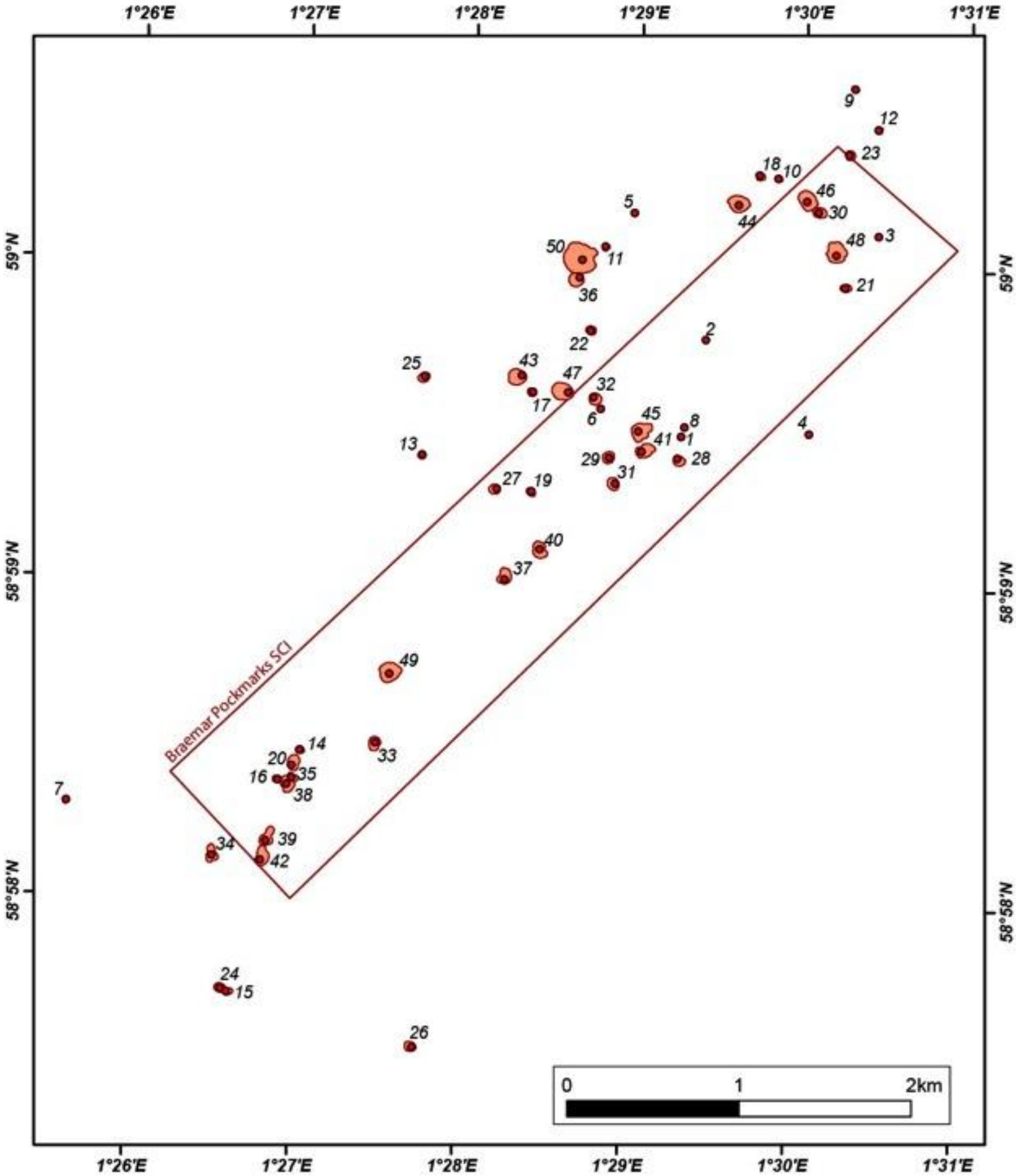

Figure 5. Outline of the depressions mapped from data from JNCC cruise CEND 19x/12 within and surrounding the Braemar Pockmarks SCI showing their identification number and their deepest point (red).

Note that all, except depression number 2, were considered to be seabed pockmarks. The depressions are numbered in order by area with the smallest numbered as 1 and the largest 50.

Table 3. Pockmark attribute table, generated by the semi-automated method.

The given values for latitude (Lat) and longitude (Long) correspond to the position of the deepest point of the respective pockmark. Area is in square meters; Perimeter, Pockmark depth (P_Depth), Maximum Water Depth (MaxWD) and Minimum Water Depth (MinWD) are in meters; Maximum Slope Angle (MaxSlope), Mean Slope Angle (MeanSlope), Longitude (Long) and Latitude (Lat) are in Decimal Degrees. Note that false-pockmark 2 is not included in the table. The pockmarks are numbered in order by area with the smallest pockmark numbered as 1 and the largest being pockmark 50. Locations are indicated on Figure 5. Pockmarks within the Braemar Pockmarks SCI are shaded light blue in this table.

ID	***Area***	***Perimeter***	***P_Depth***	***MaxWD***	***MinWD***	***MaxSlope***	***MeanSlope***	***Long***	***Lat***
1	330	65	0.4	-122.6	-122.2	4.4	1.4	1.4886	58.9916
3	405	77	0.6	-122.1	-121.5	6.1	2.0	1.5078	59.0018
4	567	87	0.6	-122.5	-122.0	6.2	2.4	1.5012	58.9914
5	626	91	0.4	-123.1	-122.7	3.7	1.3	1.4831	59.0028
6	732	97	0.8	-123.3	-122.5	4.7	2.0	1.4801	58.9925
7	756	100	0.3	-124.7	-124.4	4.0	1.0	1.4271	58.9715
8	979	112	0.4	-122.6	-122.2	3.7	1.3	1.4883	58.9911
9	1016	117	0.9	-122.7	-121.9	8.3	2.6	1.5051	59.0095
10	1070	118	1.0	-123.2	-122.2	8.8	2.9	1.4976	59.0047
11	1073	123	1.0	-123.6	-122.5	6.2	2.3	1.4803	59.0010
12	1292	130	1.1	-122.7	-121.7	8.2	2.7	1.5076	59.0073
13	1509	138	0.7	-124.6	-123.9	6.4	1.8	1.4622	58.9899
14	1614	145	0.8	-123.9	-123.1	6.5	1.8	1.4505	58.9744
15	1670	149	1.2	-127.4	-126.2	3.9	0.3	1.4436	58.9617
16	1701	149	1.0	-124.1	-123.1	5.2	2.1	1.4483	58.9728
17	1827	155	1.1	-124.3	-123.2	8.2	3.0	1.4733	58.9933
18	1880	158	1.6	-123.8	-122.2	8.2	3.2	1.4957	59.0049
19	1921	159	0.7	-123.8	-123.1	5.7	1.8	1.4733	58.9881
20	2064	174	1.7	-124.8	-123.1	8.0	3.2	1.4498	58.9729
21	2206	174	1.5	-123.6	-122.1	11.1	3.7	1.5045	58.9991
22	2360	174	0.7	-123.5	-122.9	2.8	1.0	1.4790	58.9966
23	2519	179	2.1	-123.9	-121.8	11.7	4.0	1.5047	59.0060
24	2806	191	1.0	-127.1	-126.1	8.5	2.0	1.4430	58.9618
25	2932	195	2.4	-126.1	-123.7	18.9	4.7	1.4623	58.9940
26	2952	195	1.8	-128.1	-126.3	13.9	3.7	1.4625	58.9590
27	2972	195	1.7	-125.1	-123.4	13.7	3.9	1.4698	58.9882
28	3156	203	1.0	-123.1	-122.1	6.9	2.2	1.4880	58.9900
29	3745	218	1.3	-124.0	-122.6	6.0	2.3	1.4811	58.9900
30	3812	226	2.4	-124.5	-122.1	11.9	4.5	1.5017	59.0030
31	3823	221	1.6	-124.2	-122.6	12.5	2.8	1.4818	58.9886
32	3869	222	2.0	-124.5	-122.6	13.3	3.1	1.4794	58.9931
33	4217	238	1.6	-124.4	-122.9	9.7	2.8	1.4581	58.9749
34	4944	289	0.8	-124.6	-123.8	4.7	1.3	1.4419	58.9688
35	5018	261	1.7	-124.8	-123.1	12.7	3.3	1.4497	58.9736
36	5492	264	1.4	-124.5	-123.1	11.8	1.7	1.4777	58.9993
37	5582	280	1.9	-125.4	-123.4	11.9	3.1	1.4708	58.9835
38	5866	280	2.1	-125.2	-123.1	13.4	3.3	1.4493	58.9726
39	5934	320	1.1	-125.0	-123.8	7.8	1.9	1.4473	58.9696
40	6157	295	2.2	-125.3	-123.1	10.7	3.5	1.4743	58.9851
41	6673	317	2.7	-125.1	-122.5	14.9	4.2	1.4843	58.9903
42	6729	317	1.4	-125.2	-123.8	8.2	2.2	1.4468	58.9686
43	7579	314	3.1	-126.4	-123.3	18.4	3.9	1.4721	58.9941
44	9168	355	3.5	-125.8	-122.4	13.2	4.1	1.4936	59.0033
45	9273	371	2.7	-125.1	-122.5	11.5	3.5	1.4840	58.9914
46	9406	355	4.0	-126.1	-122.1	15.2	4.7	1.5005	59.0035
47	9833	358	2.4	-125.4	-123.0	15.7	2.2	1.4768	58.9933
48	10833	395	3.7	-125.7	-122.1	15.6	4.6	1.5036	59.0008
49	10944	381	3.7	-126.8	-123.1	12.8	4.1	1.4594	58.9784
50	27157	619	5.8	-128.9	-123.1	16.5	3.7	1.4780	59.0002

Of the 49 mapped pockmarks, 27 are within the Braemar Pockmarks SCI Boundary, 21 are less than 1 km away from the SCI limits and only one, pockmark 26, is situated more than 1 km away from the boundary set for the SCI. The water depths within which pockmarks are found vary from -126.28 m to -121.54 m (Figure 6, Table 3). However most of the pockmarks are within the shallower part of that range with only 9 mapped below the 123.5m contour displayed on Figure 6.

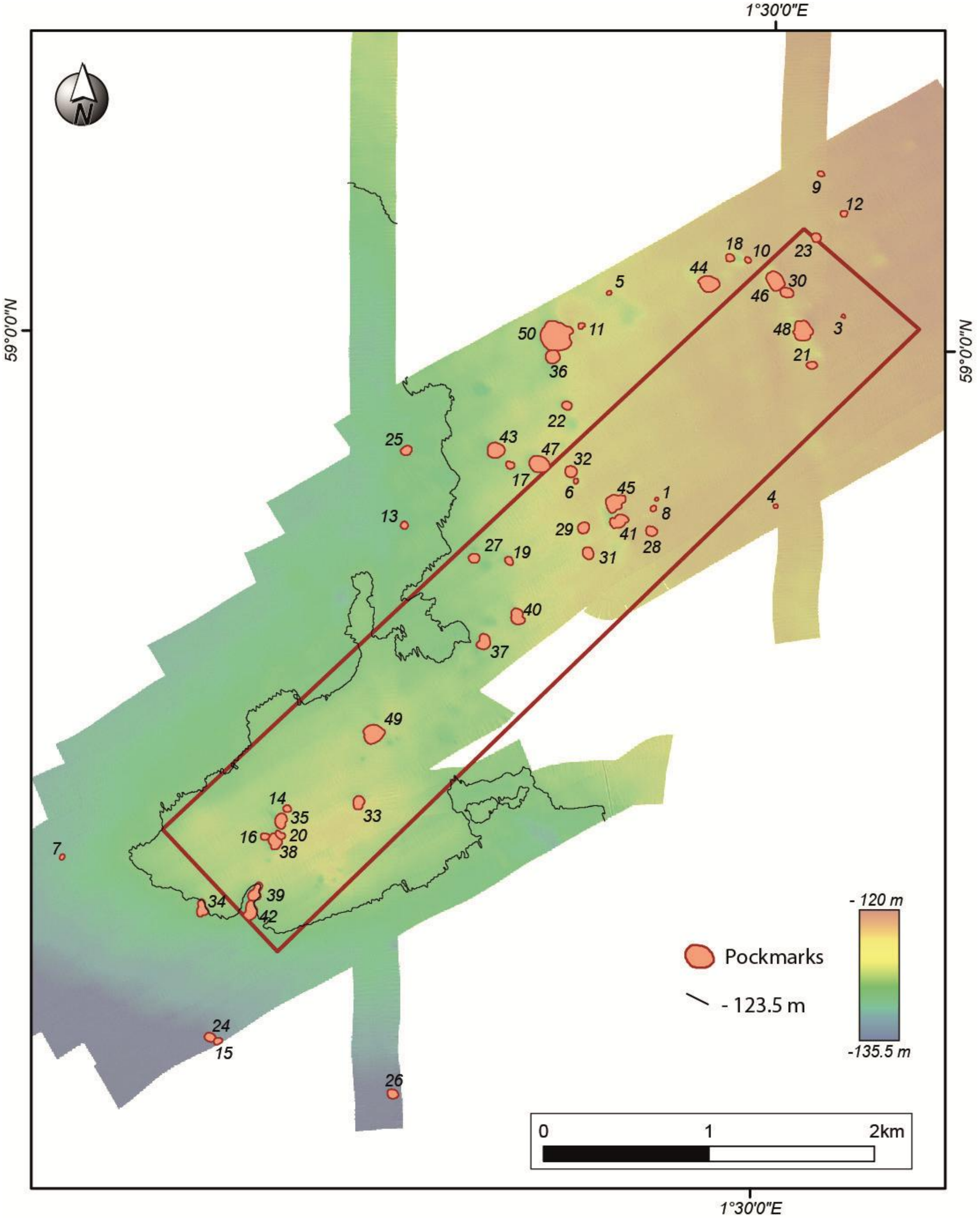

Figure 6. Outline of the 49 mapped pockmarks on the bathymetric data.
Note that the majority of the pockmarks lie in water less than 123.5 m deep.

3.3. Morphological Analysis

Most pockmarks are small to medium sized, with lengths varying from 22 m to 200 m and widths from 20 m to 189 m. Although the average pockmark area is more than 4,300 m^2, 65.3% of the pockmarks mapped are smaller than the average value (Table 3). The smallest had a surface area of little more than 330 m^2. The average pockmark area is greatly influenced by the surface area of pockmarks 48 and 49 (both greater than 10,000 m^2), and the area of pockmark 50 (with an area of over 27,000 m^2) (Table 3). In total, more than 211,000 m^2 of the seabed is affected by these gas escape features. Pockmark depths range from 0.32 m to 5.77 m, with an average of 1.65 m. Most pockmarks are between 1 m and 3 m deep; only six have a depth >3 m. These pockmarks (yellow dots on Figure 7) have dimensions comparable to individual pockmarks found in 10 other small area studies in the Witch Ground Basin (Gafeira *et al.*, 2012; areas shown on Figure 2) albeit with a wider scatter (Figure 7).

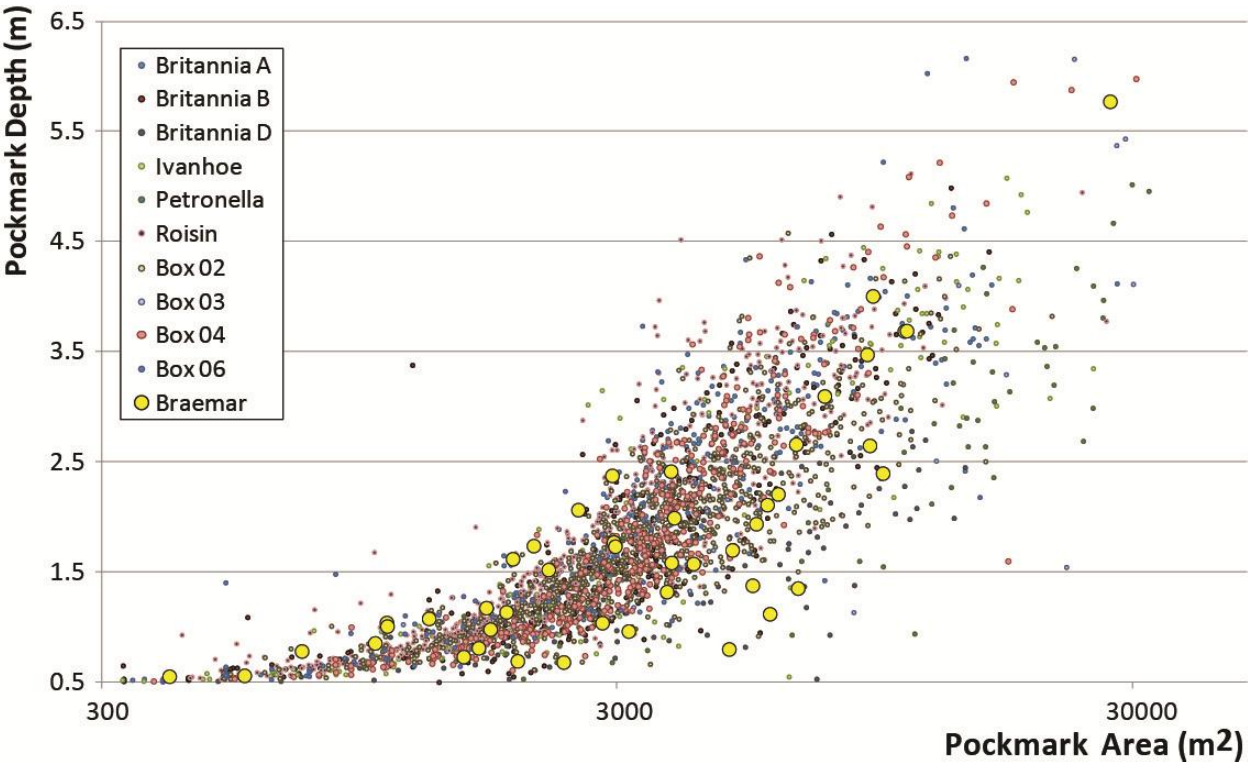

Figure 7. The relation between the pockmarks' Depth and Area for the 49 pockmark mapped on the Braemar area (yellow dots) compared to the relationship found in 10 other sites within the Witch Ground Basin (data from Gafeira *et al*., 2012).

Note that pockmarks with similar depths and area are indistinguishable. Note also the logarithmic scale used for the X-axis. Maximum depth of pockmark displayed is limited to 6.5m to show detail covering the majority of Witch Ground Basin pockmarks; this omits very deep pockmarks such as Scanner.

However, some of the pockmarks do not show the same relationship between *Area* and *Depth* found in other parts of the Witch Ground Basin (Figure 7), having shallower depths than that expected given their area. These pockmarks also do not show a circular or ellipsoid outline but have an irregular geometry in plan-view, for example the three pockmarks near the southern limit of the Braemar Pockmarks SCI boundary (34 outside the SCI boundary; and 39 and 42 inside SCI boundary; see Figure 8).

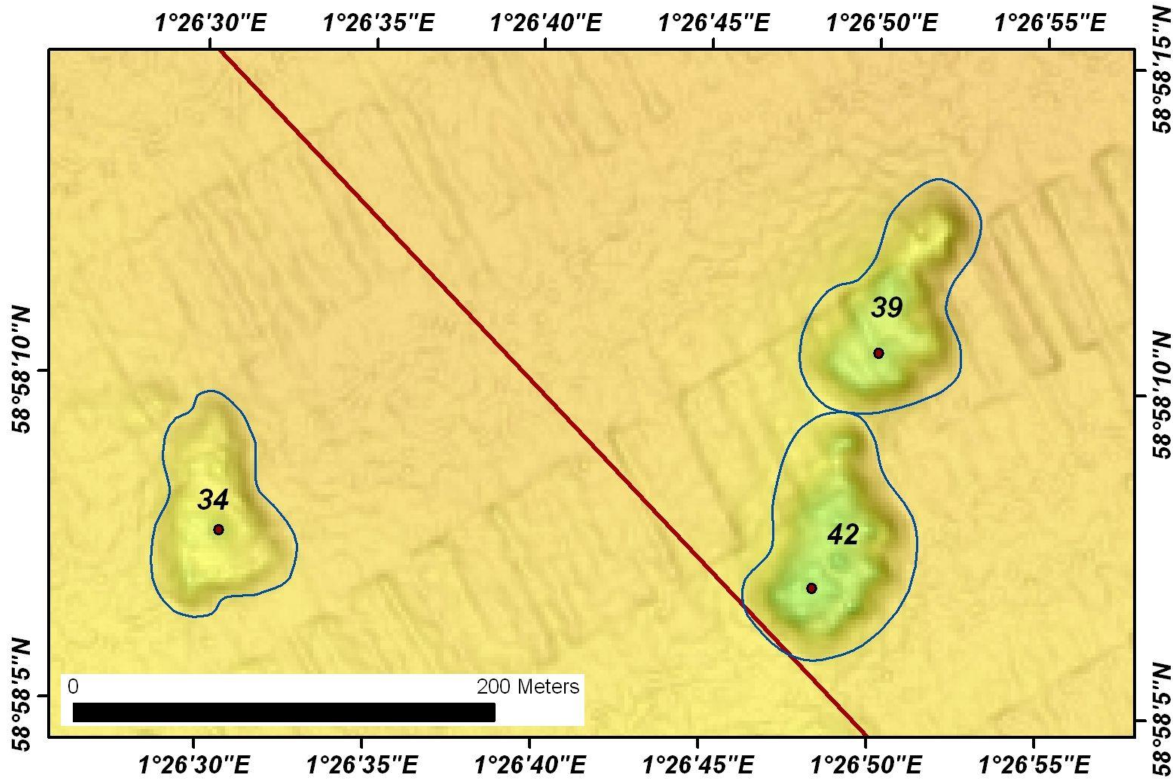

Figure 8. Shaded-relief map showing pockmark 34, outside, and pockmarks 39 and 42, inside, the red line marking the south-western limit of the Braemar Pockmarks SCI

Pockmarks have in the past been considered as typically round or elliptical in outline and 'V'-shaped or 'U'-shaped in profile (*e.g.* King in Hovland and Judd, 1988), however with the use of higher resolution survey techniques they have often been shown to be irregular in outline and their profile maybe complex or 'W' shaped. This is certainly the case for the Braemar pockmarks.

The irregular pockmark geometry may have two explanations:

1) ***Multiple vents***
   Some pockmarks appear to have multiple venting points (*e.g*. pockmarks 41 and 45; Figure 9) and are therefore compound features (*cf.* Hovland and Judd, 1988).

2) ***Sidewall slumping***
   Some pockmark present evidence of collapse of the pockmark's wall and partial infill of the pockmark bottom (*e.g.* pockmark 25; Figure 10).

Ten of the mapped pockmarks appear to have multiple venting points resulting in a 'W'-shaped profile (Figure 9). The presence of several venting points, less than 50 m apart, could be related to complex multiple flow paths for the gas to reach the seabed which may reflect intermittent seepage and blockage of flow paths. Of the pockmarks with this profile, three are outside the SCI area (pockmarks 15, 25 and 34) and seven are within it (pockmarks 20, 21, 30, 39, 41, 42 and 45).

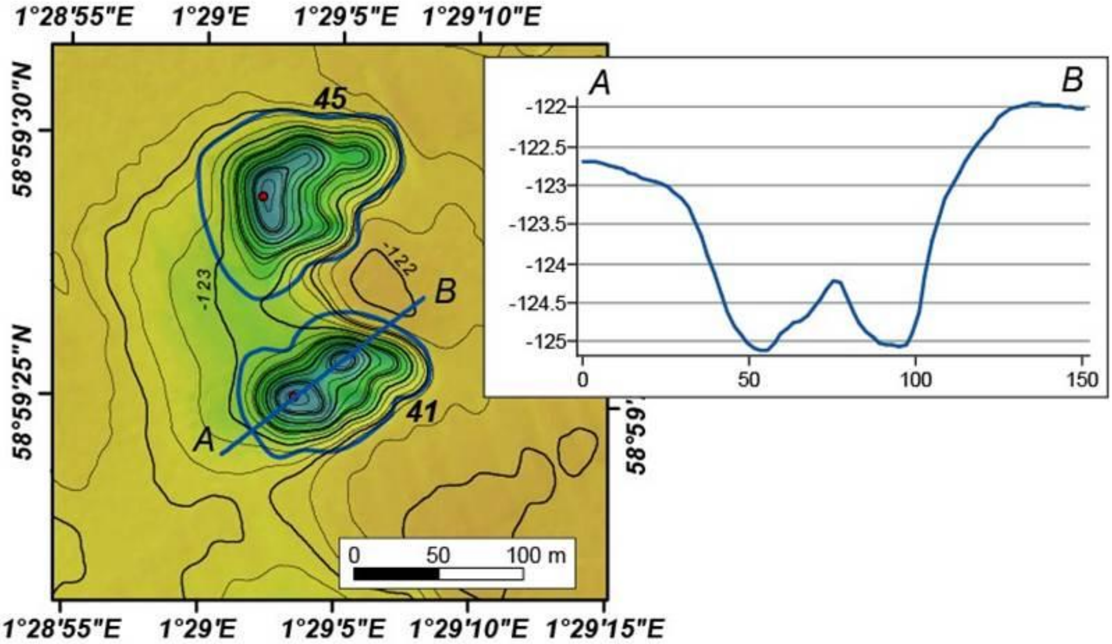

Figure 9. ***Left:*** **Shaded-relief map showing pockmarks 41 and 45.** ***Right:*** **The profile A-B across pockmark 41 shows the typical 'W' shape of the pockmark formed by multiple venting points.**

The mean pockmark sidewall slope varies between 0.26° and 4.73° (overall mean 2.77°), whereas the maximum sidewall slope varies between 2.79° and 18.95° (overall mean 9.70°). Considering that these sediments are *very soft* to *soft* with most undrained shear strengths less than 10 kPa in the upper three metres, it is not surprising that the pockmarks with the higher sidewall slopes (e.g. pockmark 25, located outside the SCI boundary) also show evidence of sidewall slumping: slope angles shallower than unaffected parts of the same pockmark, hummocky slope profiles, etc. In pockmark 25, 35% of the sidewall, on the south-western side of the pockmark, has slumped (Figure 10).

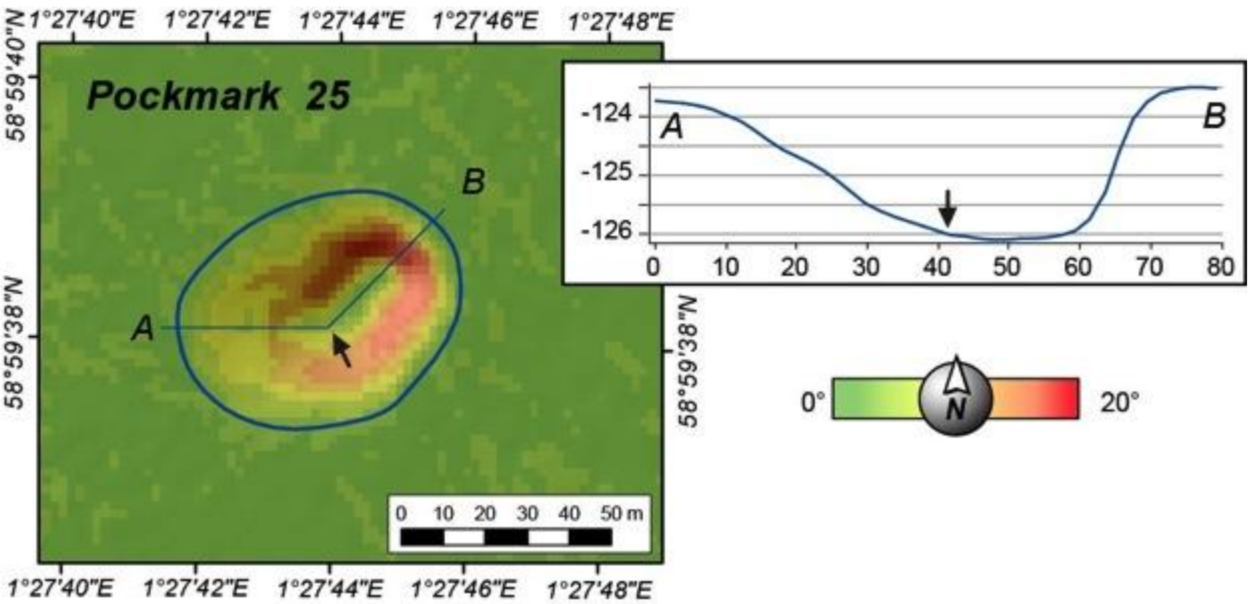

Figure 10. Detail of the slope map of pockmark 25 (*left*) and the bathymetric profile (*right*) extracted from the JNCC multibeam dataset, showing evidence of slumping on the south-western sidewall.

Due to the development of steep slopes associated with the formation of the pockmarks, the sidewalls of most pockmarks mapped in this area are potentially unstable. In fact, nearly a quarter of the mapped pockmarks present an irregular topography that could be evidence of slumping. Slope instability is only observed in pockmarks with maximum slopes of more than 10°. In some cases the material apparently remobilised only covers a small area of the flat bottom of the pockmark, however in some pockmarks it seems that more than half of the pockmark bottom is filled with slumped material. Pockmark 48 shows one of the most marked case of infilling by slumping, with more than 65% of its central area filled with remobilised material that can reach more than half a meter in thickness above the surrounding unfilled areas (Figure 11). This phenomenon of pockmark infilling has been reported from elsewhere in the Witch Ground (*e.g*. Judd *et al*., 1994).

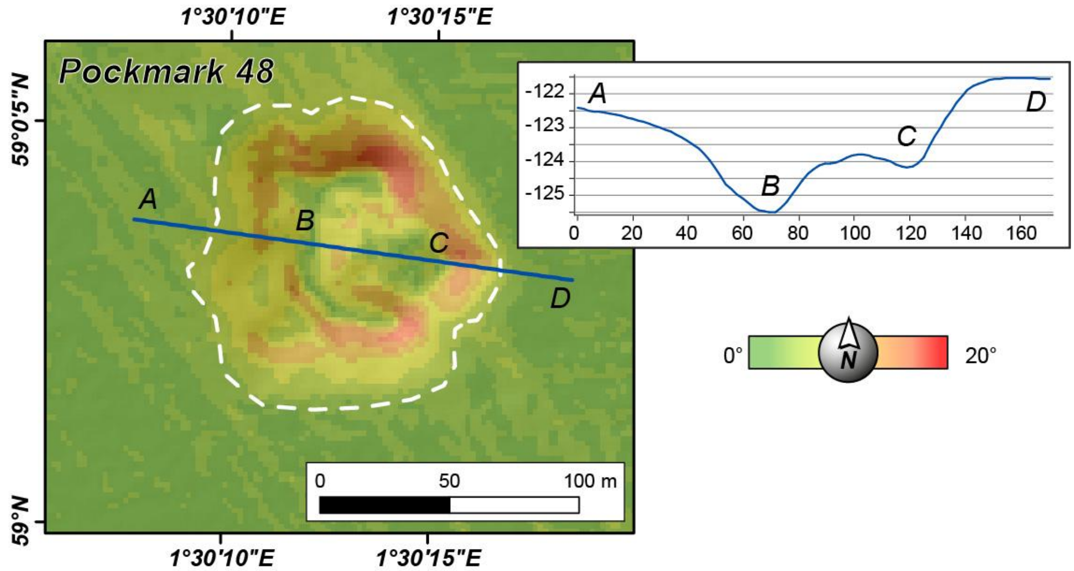

Figure 11. Slope map of pockmark 48 and bathymetric profile across pockmark 48.
Note the possible slump material between B and C.

The pockmarks affected by sidewall slumping and/or multiple venting points are identified in Appendix 2.

3.4. Surveys Comparison

One of the main tasks planned for this study (Appendix 1) was the comparison of the dataset acquired in 2012 by JNCC with available previous datasets. The purpose of this comparison was to identify any infilling or expansion of the pockmarks. An increase in pockmark area associated with a decrease in depth may indicate sidewall slumping; an increase in depth may indicate fluid escape activity.

3.4.1. Comparison with BP dataset

An analytical comparison was conducted using the ArcGIS "*Minus"* tool, which subtracted the water depth value of the BP raster from the water depth value of the JNCC raster on a cell-by-cell basis. However, the result of this subtraction revealed mainly the differences in the datasets' acquisition artefacts (Figure 12). The artefacts were mostly present in the BP dataset, possibly due to poor tidal correction.

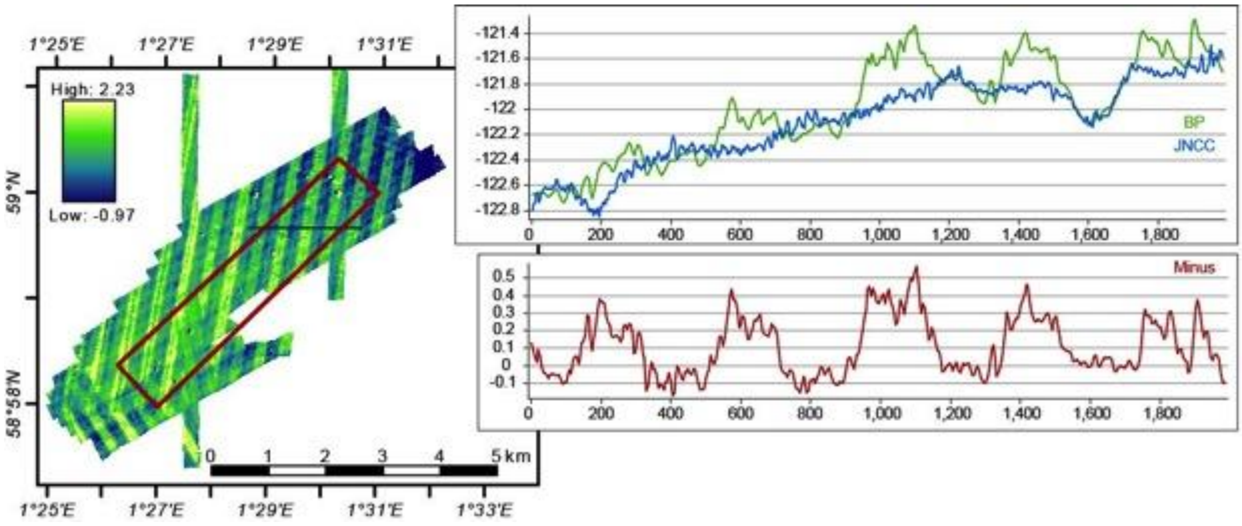

Figure 12. ***Left:*** **BP dataset minus the JNCC dataset; the presence of the acquisition footprint of the BP dataset is very marked.** ***Right:*** **Depth profiles extracted from the BP dataset (green), the JNCC dataset (blue), and the raster resulting from the subtraction of of one dataset from the other (red) along the black line marked on the map.**

To resolve the differences in observed water depth, derived rasters (a product of the pockmark semi-automated mapping method) were used. These rasters record only the value of the pockmark depth. This approach successfully reduced the differences due to vertical shifts; however it is still susceptible to horizontal shifts between the two surveys. So, the pockmark depth estimates for each individual pockmark, extracted from both datasets, were compared (Figure 13). These estimated depths should not be affected by the dataset horizontal shift. The differences between the depth estimates range from - 2 cm to 92 cm. Differences of less than 50 cm were attributed mainly to differences in cell size, the algorithms used to generate the DDMs, or to artefacts. However, differences of more than 50 cm were observed in ten pockmarks (9, 10, 15, 18, 20, 26, 32, 41, 45 and 48; Figure 13). These pockmarks were investigated further to assess if they were the result of real changes at the seabed (Appendix 3).

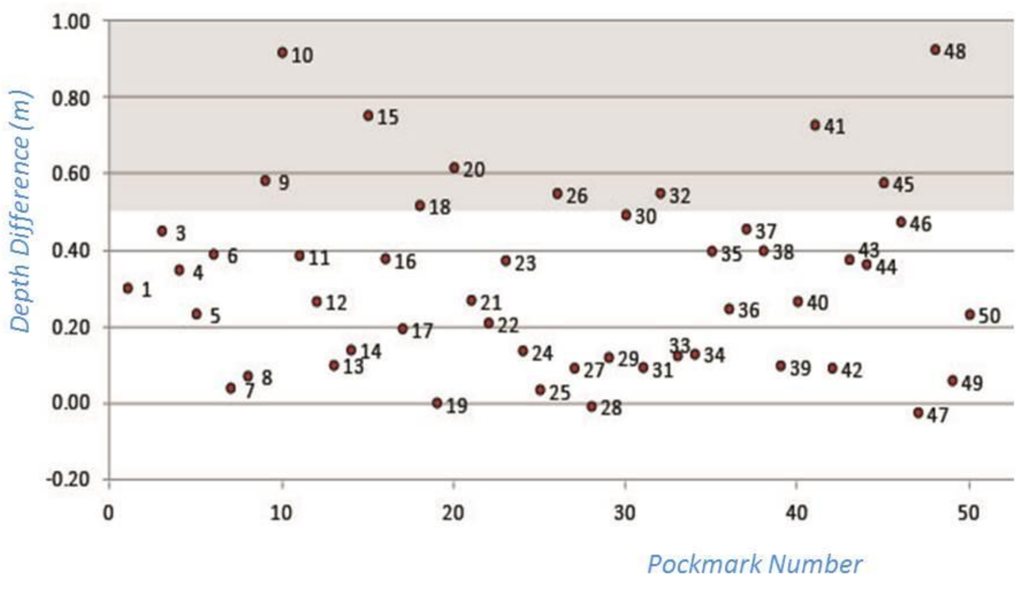

Figure 13. Difference values measured between the pockmark depths extracted from the BP and JNCC datasets.

The horizontal distance between the deepest points of each pockmark extracted from the two datasets was also measured. Most of the pockmarks showed differences of less than 12.5 meters. That is within the range expected considering both the horizontal shift observed and differences resulting from the different cell sizes and algorithms used to generate the DDMs. However, there are six pockmarks (9, 17, 30, 34, 43 and 48) for which a greater distance was evident (Figure 14). These pockmarks were also subjected to further investigation (Appendix 3).

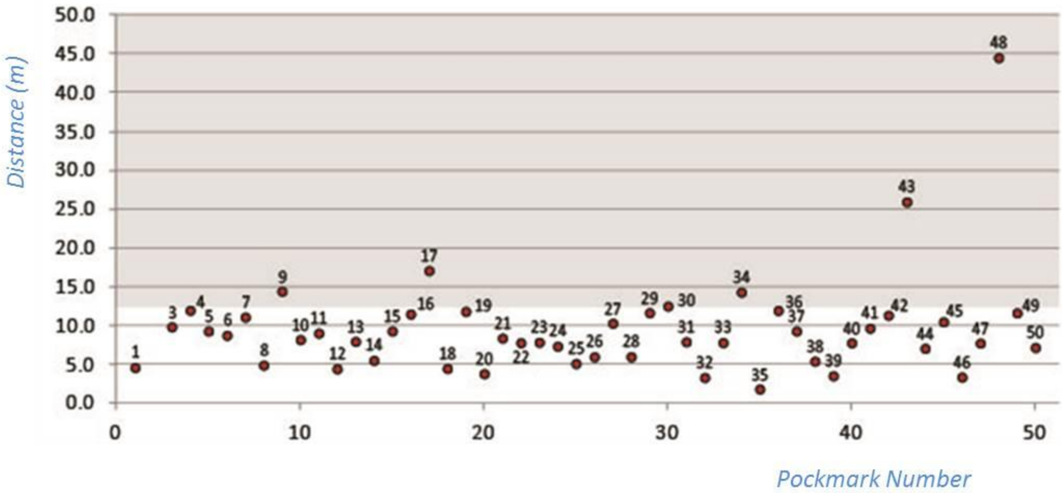

Figure 14. Distances between the positions of the deepest points, of each pockmark, extracted from the BP and JNCC datasets.

3.4.2. Comparison with Hartley Anderson Ltd desk study

As part of a desk study by Hartley Anderson Ltd for JNCC, the rig site survey for the Braemar discovery well 16/3b-8z (carried out by *Britsurvey Ltd* in 1995) was reviewed for information on pockmark features. The rig site survey included geophysical mapping of an area of 4 x 4 km centred on the proposed well site, using side-scan sonar using (100 KHz), continuous sub-bottom profiler and gravity coring at 5 locations. This survey includes areas outwith the CEND 19x/12 survey and the SCI (Figure 15), but most of the larger pockmarks mapped by Hartley (2005) are located in the area covered by the JNCC multibeam dataset.

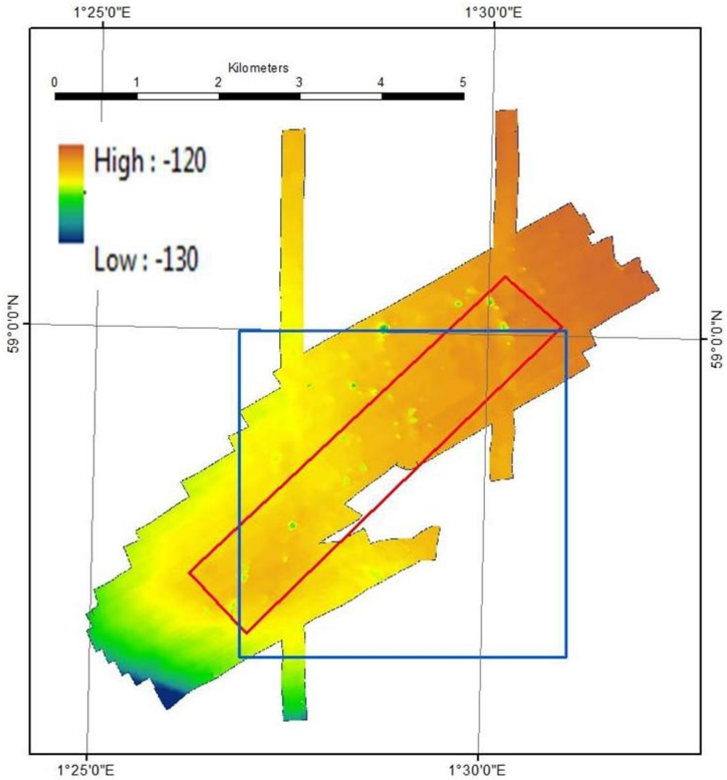

Figure 15. Comparison of Braemar SCI and area reviewed by Hartley (2005) with area of recent multibeam survey.

Limits of the site survey reviewed by Hartley (2005) are shown in blue and Breamar Pockmarks SCI limits shown in red.

Based on this dataset Hartley (2005) mapped *"Large Pockmarks"* and *"Small Pockmarks"*, areas of disturbed ground, clay exposure and gassified sediments (Figure 16). Some of the depressions identified in the JNCC multibeam data were not recognized as depressions in the earlier study (Hartley, 2005) or were described as areas of exposed clay (Table 4).

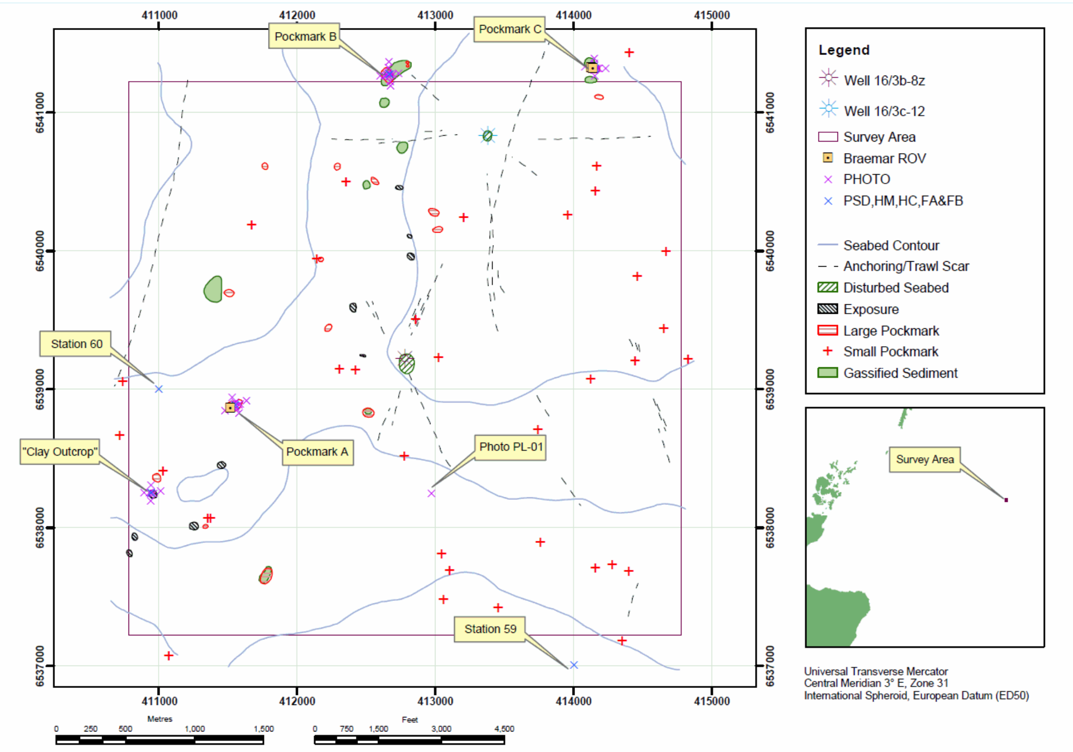

Figure 16. Interpretation of Britsurvey Ltd site survey data (Hartley, 2005).

The pockmarks mapped in that study are described as falling in two distinct size categories. The first category includes 35 pockmarks with diameters between 5 and 10 m and a maximum depth of 0.5 m. The second category consists of 18 larger pockmarks with a diameter of between 50 and 130 m and a maximum depth of approximately 5 m (Hartley, 2005). The description of two distinct size categories may suggest some type of distinction in their formation. Based on the size distribution observed in the area by the 2012 multibeam survey it seems misleading to set such a classification (Figure 17).

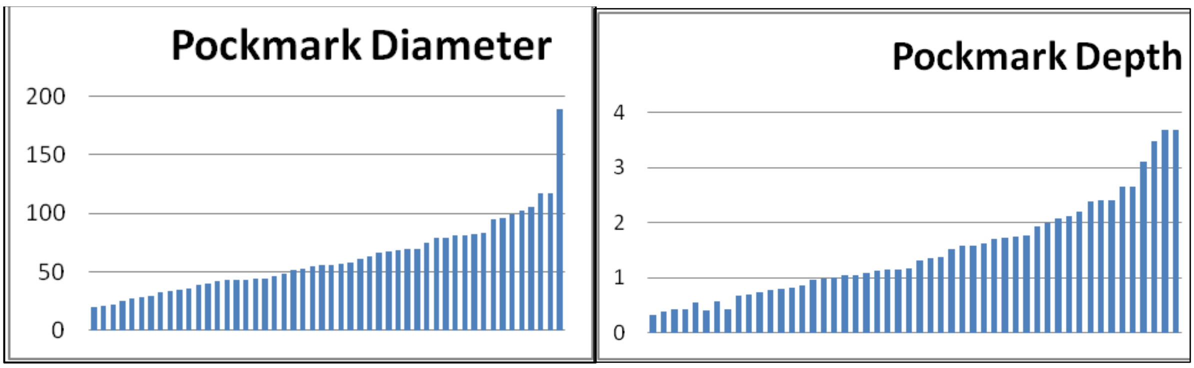

Figure 17. Pockmark diameter and depth histograms for the pockmarks mapped during the present study.

Note the histograms show a gradual increase of pockmark size that would not support any subdivision of pockmarks into two categories on the basis of size. The vertical axis in both histograms is in meters.

Table 4. Correlation of depressions mapped from the JNCC CEND 19x/12 multibeam data with how they area plotted in Hartley (2005).

Feature ID	*Mapped as in Hartley (2005)*
1	Small Pockmark
2	Well 16/3c-12
3	Small Pockmark
4	Small Pockmark
5	Outside area
6	Not mapped
7	Outside area
8	Not mapped
9	Outside area
10	Outside area
11	Large pockmark
12	Outside area
13	Small Pockmark
14	Small Pockmark
15	Outside area
16	Exposed clay
17	Small Pockmark
18	Outside area
19	Not mapped
20	Large pockmark
21	Large pockmark
22	Not mapped
23	Outside area
24	Outside area
25	Large pockmark

Feature ID	*Mapped as in Hartley (2005)*
26	Outside area
27	Large pockmark
28	Not mapped
29	Exposed clay
30	Outside area
31	Exposed clay
32	Exposed clay
33	Exposed clay
34	Outside area
35	Exposed clay
36	Not mapped
37	Large pockmark
38	Exposed clay
39	Exposed clay
40	Exposed clay
41	Large pockmark
42	Exposed clay
43	Large pockmark
44	Outside area
45	Large pockmark
46	Outside area
47	Large pockmark
48	Pockmark C Large pockmark
49	Pockmark A Large pockmark
50	Pockmark B Large pockmark

In the Hartley Anderson Ltd study, the three larger pockmarks were examined in detail including video and photographic images. These pockmarks, A, B and C, correlate with pockmarks 49, 50 and 48 respectively in this study. The pockmark areas of all three was less according to Hartley than that mapped from the JNCC multibeam in this study; this difference almost certainly reflects the different mapping approaches as well as the use of different datasets (side-scan as opposed to multibeam). A comparison between the outlines of the pockmarks should not be used to infer pockmark 'growth' when the delineation of those outlines was from two entirely different methodologies.

4. Evidence of Gas Seepage

Present day gas escape activity can be detected through direct evidence, either acoustic (e.g. strings of water column targets recorded on side-scan sonar, shallow seismic profiler or single-beam echo sounder; or MBES returns in the water column), geochemical (*e.g.* elevated concentrations of methane in the water), or visual evidence of gas bubbles entering the water column.

However, as indicated by Judd (2001): *"the observations of actual seepage could be fortuitous, chancing upon an event that is part of an intermittent process"*. Therefore, the observation of other indirect evidence can play an important role in recognising areas of seepage. Various types of indirect evidence for gas seepage have been suggested (Hovland *et al*., 2012). The most common are:

- presence of methane-derived authigenic carbonate (MDAC);
- presence of bacterial mats on the seabed;
- changes in the extent or character of shallow gas accumulations.

The occurrence of MDAC is specific evidence of methane seepage at some point in the past, but does not necessarily imply extant gas escape. However, it does imply that seepage has occurred over a prolonged time period. The presence of bacterial mats implies the presence of hydrogen sulphide in the seabed sediments, and therefore suggests anaerobic methane oxidation, on the condition that the bacterial mats are correctly identified as thiotrophic. Likewise, the presence of bacterial mats is thought to indicate seepage that has been continuous for a period of time to allow a biological community to colonise the site (Judd and Hovland, 2007). Changes in shallow gas accumulations could be the result of either an isolated leakage event or from continuous seepage.

4.1 Direct Evidence of Gas Seepage

4.1.1 Acoustic evidence

Bubbles emerging from the seafloor can be detected acoustically. The impedance contrast between gas and water is high, so reflections will be strong at most seismic frequencies, except for low frequencies, where the wave-length is too large for bubble detection this relates to the fact the size of the bubble detected is dependent on the frequency of acoustic source. Note that the gas in fish bladders can produce a similar effect as gas in the water column and is the basis for "fish-finder" equipment.

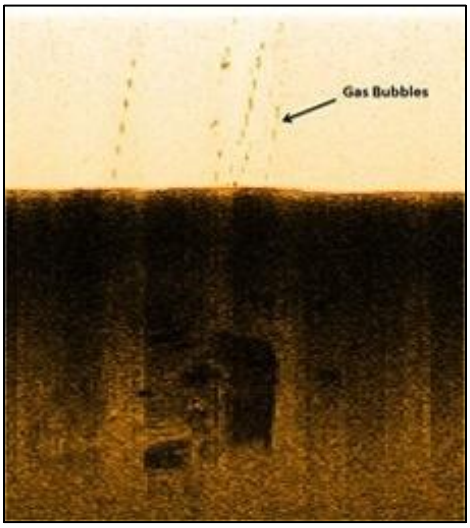

During cruise CEND19x/12, several acoustic anomalies interpreted to be due to streams of bubbles (gas flares) were encountered in the water column near pockmark 45 (Figure 18), Backscatter acoustic anomalies observed nearby on both side-scan and backscatter datasets. The flares are observed on data uncorrected for slant-range, as slightly inclined features.

Figure 18. Side-scan sonar data recording separate acoustic targets rising into the water column from pockmark 45.

Image extracted from the CEFAS & JNCC report (2013).

4.1.2 Geochemical evidence

Seepage can be identified by chemical anomalies, elevated levels of dissolved gases, in the water column above, and in the sediment pore-water system beneath the seabed. These occur when the free gas bubbling through the water column starts to exchange gas molecules with the surrounding water and may cause a strong concentration gradient of the leaking gas, with highest concentration adjacent to the stream of bubbles and reducing outwards in a radial aureole pattern. Because the rising plume of bubbles is influenced by currents, this chemical concentration anomaly will be highest down-current (Hovland *et al*., 2012). Within the sub-surface sediments, the same will occur, and there will be a concentration gradient in the pore-water surrounding the conduits transporting gas through the sediments. This gradient will be dependent on the porosity and permeability of the sediments (Hovland *et al*., 2012).

To detect geochemical anomalies within the water column would have required the collection and analysis of water samples, using for example Niskin bottles. Indirect evidence may be indicated by CTD (conductivity salinity/ temperature/ depth) measurements. To detect this type of anomaly within the seabed sediments would have been required pore water analysed from collected cores.

4.1.3 Visual evidence

Visual evidence of gas seepage can be obtained by seabed video observation of escaping bubbles. These would validate the acoustic interpretation. However, none of the videos recorded during the cruise captured images of bubble release at the seabed.

4.2 Indirect Evidence of Gas Seepage

As stated above there are several datasets that can suggest the presence of gas migration in the shallow section upwards towards the seabed before there is the opportunity to detect the migration of gas directly. These include acoustic profiling of the shallow section, particularly with higher frequency instruments such as pinger and boomer to provide high resolution records. Just as the gas reaches the seabed it may be captured and altered and the presence of MDAC or bacterial mats is evidence for this.

4.2.1 Shallow gas accumulations

Acoustic turbidity has been recognised in shallow seismic profiles and is often interpreted to be caused by free gas within sediment pore spaces. Acoustic energy is absorbed and scattered by the gas bubbles casing chaotic reflections (Judd and Hovland, 2007), albeit similar effects may be caused by layers of gravel including shells. No shallow seismic profiles were collected during the JNCC survey that might have shown changes in extent of shallow gas indicators, but BGS's regional mapping (Figure 3) involved the acquisition of shallow seismic data. The BGS data shows evidence (acoustic turbidity etc.) that is consistent with the presence of gas within the shallow sediments in the area (Figure 19). The acoustic feature beneath pockmark 46 (Figure 19, detail) is suggestive of a vertical gas migration pathway.

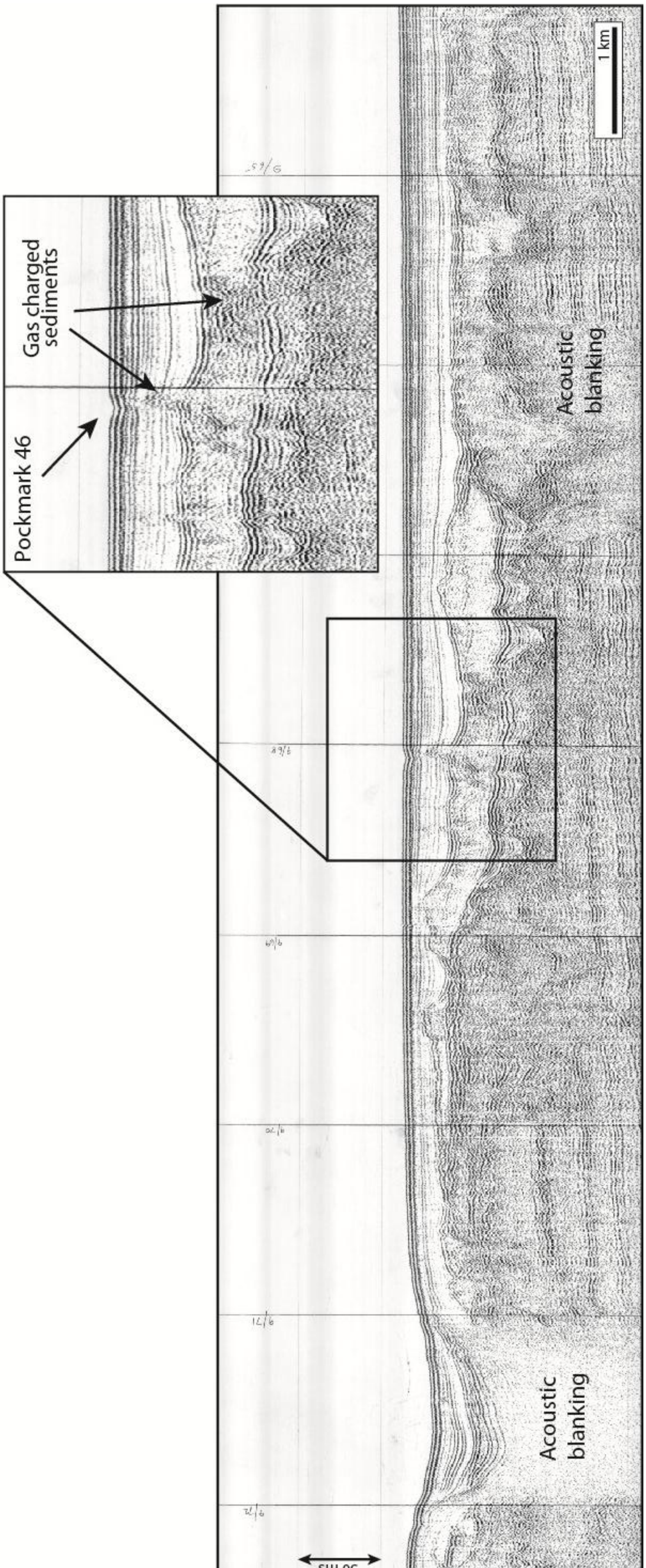

Figure 19. Sparker profile BGS 82/4 Line 9 between subfixes 64.1 and 72.4.

It shows several areas of acoustic turbidity interpreted as being due to the presence of free gas within the sediments. Inset shows detailed view of profile across pockmark 46 where acoustic anomalies under the pockmark are indicative of the presence of gas and a gas migration pathway. See Appendix 5 for location of profile.

4.2.2 Methane-Derived Authigenic Carbonate

Methane-Derived Authigenic Carbonate (MDAC) has been described from continental shelves around the world at sites of gas seepage (Judd and Hovland, 2007). MDAC generally comprises carbonate minerals (high-Mg calcite, dolomite and aragonite) which cement the normal seabed sediment to form a hard substrate. MDAC was first identified in the North Sea in 1983 (Hovland and Sommerville, 1985; Hovland *et al.*, 1987). These carbonate cements are precipitated at seepage locations as a result of the anaerobic oxidation of methane (Boetius *et al*., 2000) which usually takes places just below the seabed surrounding the gas seepage conduits (Hovland *et al*., 2012). However, fluid escape remobilizing the seabed sediment can expose the carbonate.

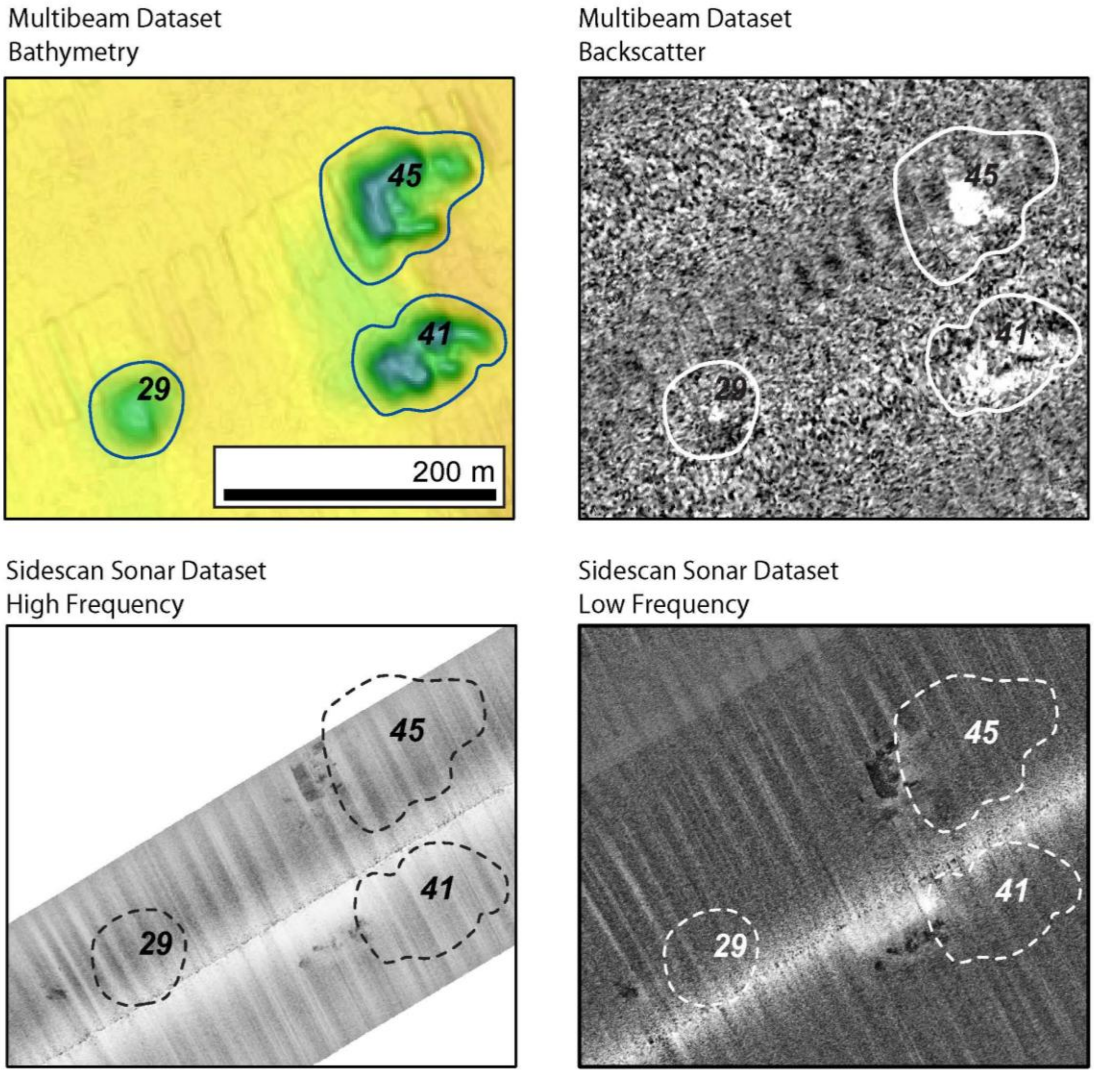

Figure 20. Comparison of seabed imagery obtained from different acoustic systems during the cruise CEND19x/12, covering the pockmarks 29, 41 and 45.

Note that the patches of high reflectivity seen in both side-scan sonar datasets are displaced by 65 – 70 m from their equivalent on the multibeam backscatter data as a result of incorrect towfish layback correction. Note also that areas of high backscatter appear white on multibeam backscatter but black on side-scan sonar.

Due to its hardness, MDAC may be detected by acoustic systems (*e.g.* side-scan sonar (SSS) and multibeam echo sounder (MBES)) where it produces a stronger acoustic reflection than the surrounding, uncemented seabed sediments. However, ground truthing provided by visual observation or seabed samples are more reliable evidence of the presence of MDAC exposed at seabed, as a change in sediment particle size or the presence of shell hash, both characteristic of pockmarks, could also produce higher backscatter, albeit not as strong as that from cemented sediments. If samples are collected only then the presence of MDAC can be confirmed by mineralogical, chemical and isotopic analysis. Such analysis was undertaken on some samples (Milodowski and Sloane, 2013).

During the comparison of multibeam and side-scan backscatter signatures, it could be clearly seen that the 'seabed response' is dependent on the geophysical method and that there are positioning discrepancies of tens of meters (Figure 20). The high backscatter areas in the side-scan images, (with both *High* and *Low Frequency*) are found 65-70 meters from their equivalent on the multibeam dataset. No major differences were detected between the side-scan sonar images derived from the different frequencies. The multibeam generally indicates more extensive areas of strong backscatter. This may be a function of the differing geometry of the incident acoustic signals, the horizontal resolution of the systems, and/or differences in seabed penetration caused by the different acoustic frequencies (although is considered to be negligible as the frequencies are similar).

On the multibeam dataset, more than two thirds of the pockmarks mapped showed areas of significant high backscatter (*e.g.* pockmarks 41 and 45 on Figure 20). Of the pockmarks with limited acoustic anomalies (*e.g.* pockmark 16), there are actually very few that do not show any acoustic anomaly (*e.g.* pockmarks 22 and 47). The absence of identifiable patches of high backscatter may be due to noisy data on the edges of the multibeam, the presence of MDAC at depth (below penetration of the MBES or SSS), or the absence of MDAC. Pockmarks with high backscatter patches are identified in Appendix 2.

The interpretation that high backscatter on MBES and/or SSS is correlated to seabed exposures of a rock-like substance is validated by the video images obtained during the cruise (Figure 21), and the seabed samples that recovered fragments of rock. A total of 11 samples recovered MDAC, from six individual pockmarks (35, 38, 40, 48, 49 and 50), as reported in Milodowski & Sloane (2013). Pockmark 42 was the only pockmark sampled that failed to recover rock material. Nevertheless, the acoustic data from this pockmark is consistent with the presence of carbonate on the seabed.

Figure 21. Example photograph (Stn11 026) showing scattered carbonate coverage.

Still image (Stn11 026) was capture within Pockmark 40 (1° 28' 26.724" E; 58° 59' 6.144" N), a few metres from where grab samples HG08 37B and HG08 37C (with fragments of MDAC) were taken.

4.2.3 Seep-Associated Fauna

4.2.3.1 BACTERIAL MATS

As a result of strong chemical gradients at seepage locations, microorganisms such as archaea and bacteria can flourish at such sites. The most common visible microorganism found at marine methane seep sites, the world over, is the thiotrophic bacterium *Beggiatoa sp* (Hovland *et al.*, 2012). This, and also many other types of bacteria, can produce thick mats on the seafloor. However sampling, and subsequently culturing of the species, needs to be undertaken to confirm the presence of Beggiatoa.

At Braemar SCI the ROV video inspection transects made across pockmark 49 in 2003 (pockmark A of Hartley, 2005) observed white bacterial mats, possibly of *Beggiatoa sp.*, on the seabed. Bacterial mats were again recorded in the same pockmark by Envision in their interpretation of the video and stills collected by JNCC cruise CEND19x/12 at Stn 10 (Figure 22).

Figure 22. Bacterial mat (white) observed in Pockmark 49 (Photo: BRMR 25 Stn 10_120).

4.2.3.2 BIVALVES WITH SYMBIONTS

Some fauna have a symbiotic relation with microorganisms that derive their energy from chemosynthesis and which then in turn support higher order species such as bivalves.

Dando (2010) noted that only four of 173 macro fauna species (*Siboglinum fiordicum*, *Lucinoma borealis*, *Axinulus croulinensis* and *Thyasira equalis*) found in three of the Braemar pockmarks by Hartley (2005) had symbionts and that none of these were restricted to seeps but could be found in normal reducing environments.

5. Sedimentation

This part of the North Sea has had negligible sedimentation at the present time and such conditions are likely to have been similar since early Holocene times. Active sedimentation ceased after the retreat of ice sheets. The most recent sediments are the late glacial Witch Ground Formation (Figure 23). The Witch Ground Formation (WGF) is a late glacial to Holocene seismo-stratigraphic formation whose sediments covered ice-scoured depressions and comprise muds, sandy muds and muddy sand often with organic debris (Johnson *et al*., 1993). Within the upper 3 m, these sediments are *very soft* to *soft* with most undrained shear strengths less than 10 kPa. Geotechnical data from a nearby pipeline survey indicate the WGF sediments to be of non or low plasticity (PI<15) meaning fractures could develop easily by buoyant gas bubbles, thereby aiding fluid flow. This formation is recognizable on seismic profiles as being acoustically well layered upon an irregular basal surface. Its upper surface is the present day seabed. Acoustic turbidity is a common feature of the WGF and is generally attributed to shallow gas (Judd, 2001; Judd and Hovland, 2007).

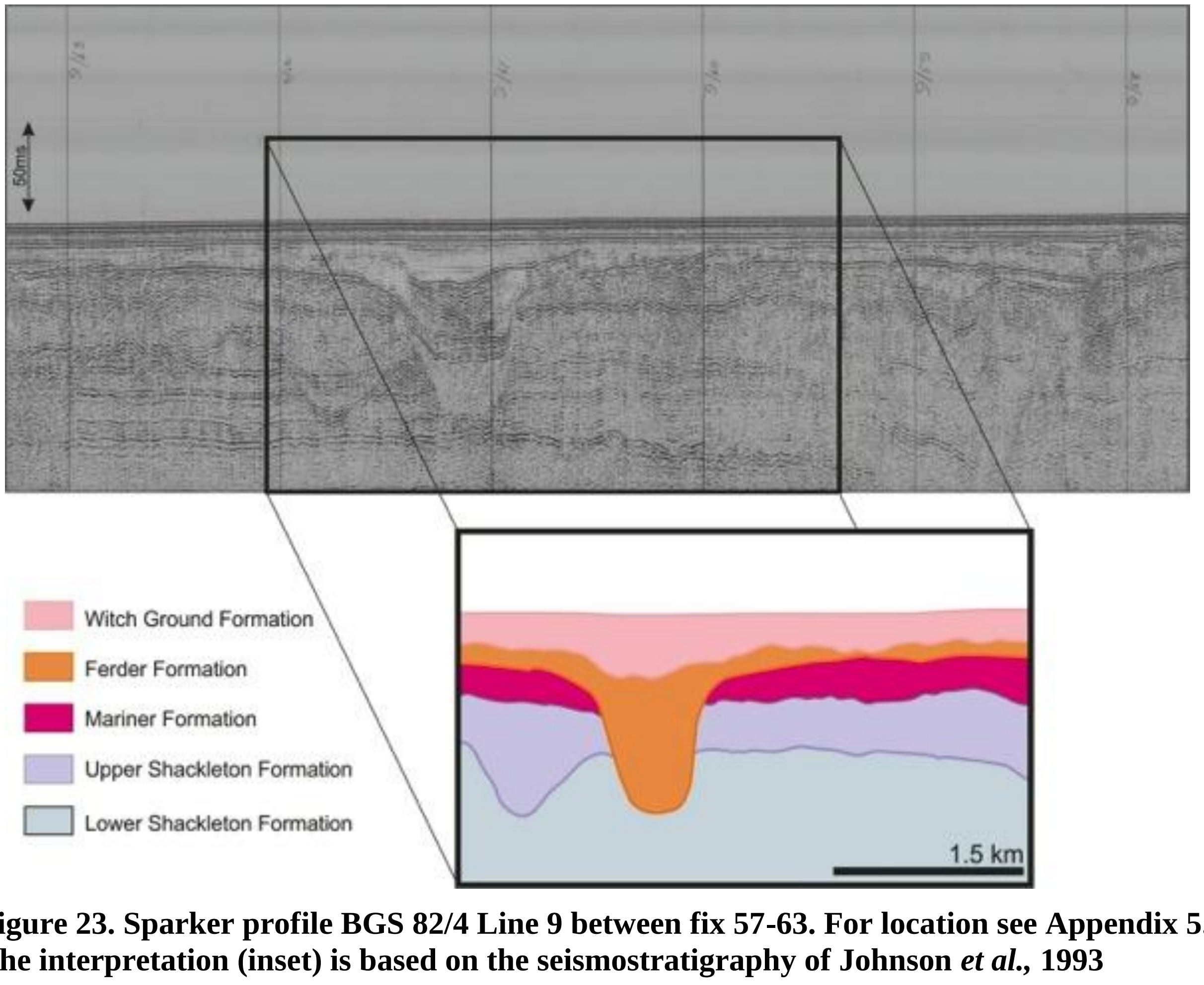

Figure 23. Sparker profile BGS 82/4 Line 9 between fix 57-63. For location see Appendix 5. The interpretation (inset) is based on the seismostratigraphy of Johnson *et al.*, 1993

The Braemar site lies towards the edge of the Witch Ground Basin where the WGF sediments are coarser than they are closer to the centre of the basin.; BGS samples 58+01/65 and 58+01/136, located adjacent to the SCI boundary limits (Figure 2), and the shorter penetrating grab samples collected by JNCC within the SCI, show that the WGF sediments comprise silty sand. This is in contrast to the WGF at Scanner where it comprises muds. This difference in lithology may influence the differences in pockmark size and geometry between the pockmarks of the Braemar and Scanner SCIs; and may make slope failure more likely. Also the increased permeability and reduced plasticity will enhance fluid flow.

The environmental history of the area has been controlled by climatic changes since the last glacial maximum about 18,000 years ago. At that time the area was buried under ice many hundreds of metres thick, however, as warming began the ice sheet started to melt away and eventually allowed a marine incursion from the north to occur (Bradwell *et al.* 2008). Before 15,000 years ago, the area was probably a small shallow sea with a near permanent sea-ice cover. The sea was probably no larger in extent than the present WGF. The sea ice, together with small icebergs, transported sediment from the flanks of the basin in to the central area. The seabed was continually being re-worked by the ploughing of ice keels, and locally, ice loading, causing overconsolidation of the underlying sediments. During periods of low temperature it is likely that permafrost occurred, creating lenses of ground ice extending from adjacent land areas (Long, 1991)

As the temperature began to rise, about 15,000 years ago, sea level rose slightly, the sea ice became thinner, and the seabed ceased to be disturbed by the ice keels. This transition is represented by the irregular base of the WGF where the last sea-ice plough marks are preserved (Stoker and Long, 1984). Between about 15,000 and 13,000 years ago, rapid sedimentation beneath a cover of sea ice took place, forming the acoustically well-layered Fladen Member of the WGF (Long *et al.*, 1986; Long, 1992).

About 13,000 years ago, the cold polar front was moving rapidly northwards past Britain, permitting the entry of warmer North Atlantic waters into the North Sea. Palæontological evidence (Long *et al.*, 1986) suggests a rapid rise in temperature with only limited sea ice. Such a rise in bottom water temperatures is also likely to have rapidly melted any sub-surface lenses of ground ice.

Marine sedimentation continued, with the short-term return of sea ice during the Younger Dryas (Loch Lomond) period (circa 11,000 to 10,000 years ago; Long *et al.*, 1986). Radiocarbon dating of seabed sediments in the Witch Ground suggests that there has been virtually no sediment input since the early Holocene, about 8,000 years ago (Erlenkeuser, 1979 & pers. comm. 1988; Johnson and Elkins, 1979). Sedimentation today is restricted to the formation of the Glenn Member of the WGF through re-working of the Witch Member during pockmark formation. Gas escape during pockmark formation sorts the near-surface sediment in such a way that a very thin layer of very well-sorted silt forms, thickening into individual pockmarks (Stoker *et al.*, 1985; Andrews *et al.*, 1990).

Early attempts at dating sediments in the central North Sea involved whole sediment radiocarbon analyses (Holmes, 1977), which has the potential to incorporate “old carbon” thereby generating an inaccurate age. There have been only a few actual radiocarbon datings to calibrate the geological model created for the WGF. These include a series of dates from a core (58+00/111VE) taken near the centre of the basin, 58°35'N 00°30'E (Hedges *et al.*, 1988). Although the dates are not in sequence, they suggest very rapid sedimentation around 13,600 years ago (D. Long comment in Hedges *et al*., 1988). They underlie a horizon (0.4 – 0.6 m depth) containing shards of volcanic glass correlated with the Vedde Ash event of ~10.6 ky. This site, and site BH81/26 (58°08.34'N, 0°10.63'W) which has shards from the same event (Long and Morton, 1987), indicate that there was a sudden change in sedimentation rates following the Younger Dryas episode and the onset of the Holocene at 10,000 years ago, giving a sedimentation rate of ~5 cm/ky . This is supported by a gastropod at 27 cm depth with an age of 4780±130 years BP giving a sedimentation rate of 5.6 cm/ky (Johnson and Elkins, 1979) for a core located at 58°25.5'N, 0°40'E (Elkins, 1977). Similar radiocarbon ages have been obtained at similar depths in a couple of cores analysed by Erlenkeuser (1979) supporting a reduced sedimentation rate during the Holocene (the last 10,000 years) but suggesting that sedimentation ceased around 2,000 years ago (Figures 24 and 25).

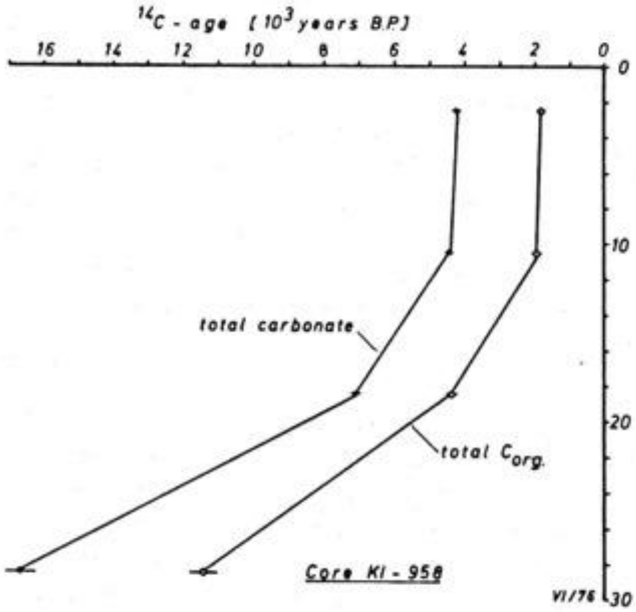

Figure 24. Profile of core Kl-958 in 146m water depth, Witch Ground Basin (Erlenkeuser, 1979).

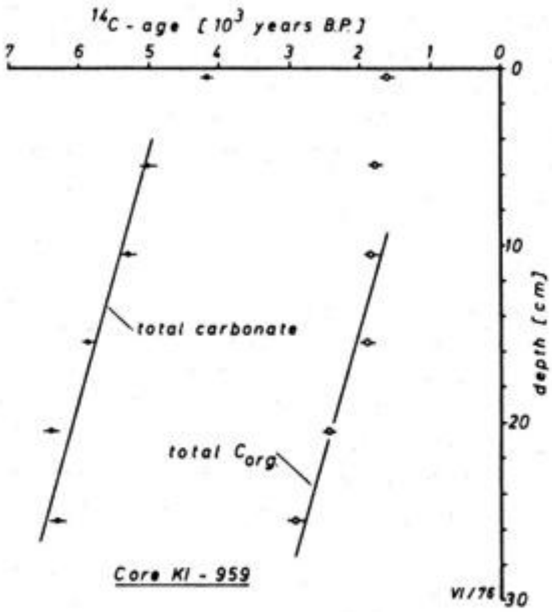

Figure 25. Profile of core Kl-959 in 125m water depth, Witch Ground Basin (Erlenkeuser, 1979).

6. Anthropogenic Activities

The main potential sources of human physical disturbance of the seabed and foreseeable effects are summarised below, followed by considerations as to whether these could adversely affect the integrity of the Braemar Pockmarks SCI and the designated features within.

6.1. Oil and Gas Exploration and Production

The Braemar Pockmarks SCI's name originates from its proximity to the Braemar Field (Figure 26). The Braemar Field is a small gas and condensate reservoir discovered in 1985 (discovery well UK 16/3b-8) and located in UK Continental Shelf Block 16/3c. The field was developed by BP (development approval granted 2002), with a single cased well tied back to the Marathon-operated East Brae platform 12 kilometres (7.5 miles) to the south where the liquids and gas are processed (Figure 26). BP sold its holdings and the operatorship to Taqa Britani in 2012. The Braemar field held initial estimated recoverable reserves of 3.28 billion m^3 of gas and 1.59 million m^3 of condensate. According to DECC data, by September 2012, the cumulative production had already exceeded these estimated recoverable reserves and production is ongoing.

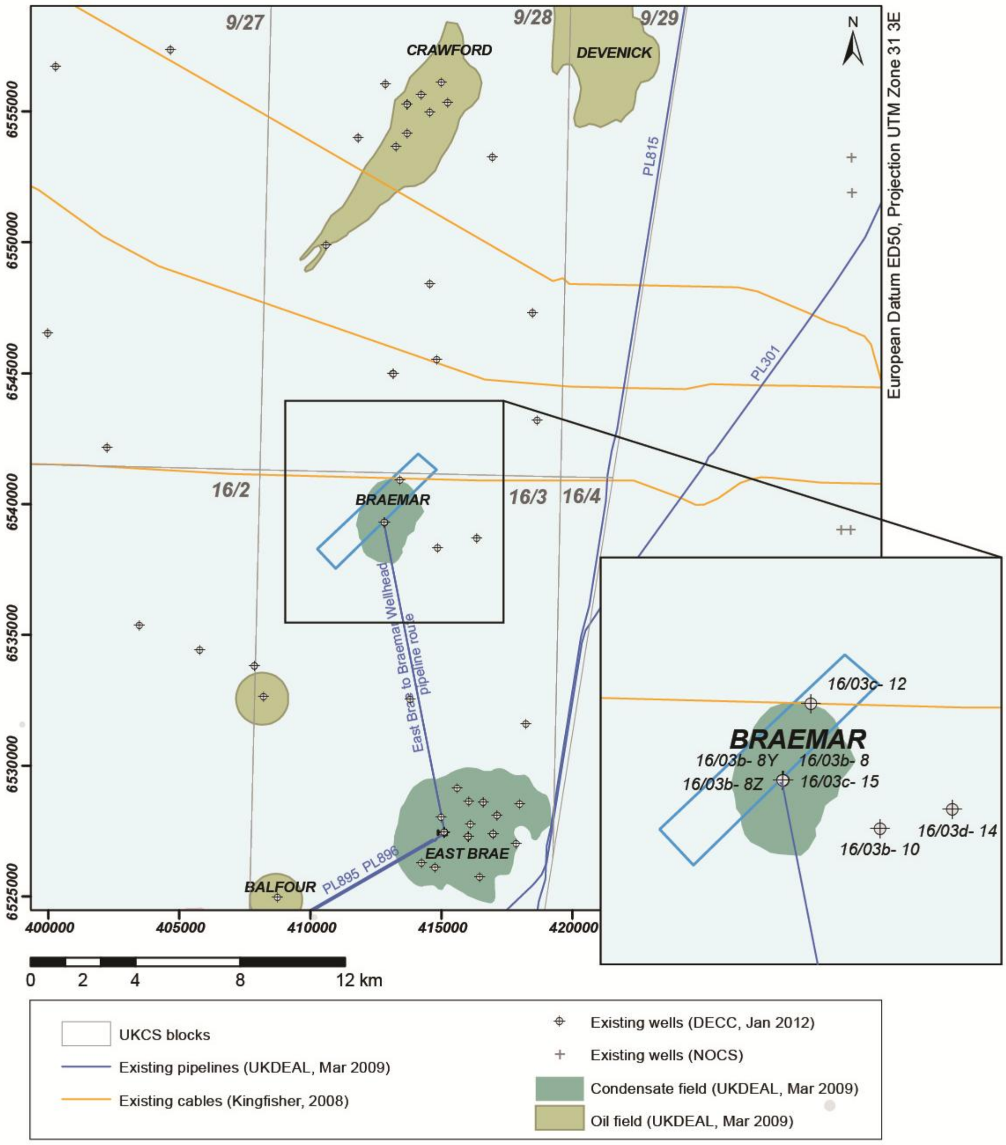

Figure 26. Oil fields and subsea infrastructure features in the vicinity of the Braemar Pockmarks SCI.

Several activities associated with oil and gas exploration and production can lead to physical disturbance, damage, alteration or contamination of seabed habitats and geomorphological features, with consequent effects on benthic communities. According to the environmental assessment published by DECC (2013) prior to the 27th Seaward Licensing Round, the main sources of physical disturbance of the seabed from oil and gas activities near the Braemar Pockmarks SCI are:

Anchoring of semi-submersible rigs: Semi-submersible rigs use anchors to hold position, typically between 8 and 12 in number at a radius depending on the water depth. The use of anchors and chains or cables can cause seabed disturbance and some re-suspension of sediments, and 'anchor mounds' could be left after their retrieval in cohesive sediments. The water depths in the area are considered too deep for a jack-up rig to be used.

Drilling of wells: The tophole sections of exploration wells are typically drilled riserless, producing a localised (and transient) pile of surface-hole cuttings around the surface conductor pipe. The installation of the surface casing and blowout preventer may result in physical disturbance of the immediate vicinity (a few metres) of the wellhead. Once the casing has been installed the drilling of wells is unlikely to be a source of sediment or disturbance to the seafloor.

Production platform jacket installation: Limited physical footprint similar to a drilling rig, but present on site for longer periods.

***Subsea template and manifold installation*:** Limited physical footprint at seabed, smaller than a drilling rig, but present on site for longer periods.

Pipeline, flowline and umbilical installation, trenching and potentially, placement of rock armour: Large pipes (greater than 16" diameter) do not have to be trenched according to a general industry agreement as they will not be moved by fishing gear, but they may still need to be trenched for reasons of temperature loss or upheaval buckling (due to buoyancy). Smaller pipes will need to be trenched to avoid interaction with fishing gear dragged along a seafloor. Trenches may require several passes before they are of the required depth of burial. Or if it is impossible to achieve the required depth due to obstructions, in which case rock is usually placed on the pipeline (rock dump) to protect and stabilise it. Rock dumping may also alleviate the hazard of free-spanning within the pockmark.

Oil and gas exploration and production activities result in marine discharges that include produced water, sewage, cooling water, drainage, drilling wastes and surplus water-based mud; the latter may contain remnant particulate oil (in droplet form), dissolved oil, organic acids, phenols, metals, production chemicals, and radioactive material (DECC, 2013). Produced water is the largest-volume marine discharge for offshore oil and gas production activities. Several toxicity studies of produced water *(e.g.* Berry and Wells, 2004) have concluded that the necessary dilution to achieve a *No Effect Concentration* would be reached at <10 to 100 m and usually less than 500 m from the discharge point depending on the currents and water stratification, consequently current production activity is not likely to affect the SCI.

There are no seabed monitoring surveys associated with wells drilled at Braemar within the publically accessible UK Benthos dataset. However data gathered from monitoring the nearby well 16/3d_14 (Table 5, Appendix 4) are available. These show elevated hydrocarbon readings on seabed sediments and provide a useful analogue for sediment movement near the Braemar Pockmarks SCI. Hydrocarbons are presumed to be mainly spread with the drill cuttings from drilling the tophole section of the well, assuming that traces of hydrocarbons occur in the tophole section or that the hydrocarbons are derived from oil-based drilling muds or other additives. Figure 27 and Figure 28 show that the high concentrations of hydrocarbons are only found up to 200 m from the site, which suggests that sediment migration is relatively short.

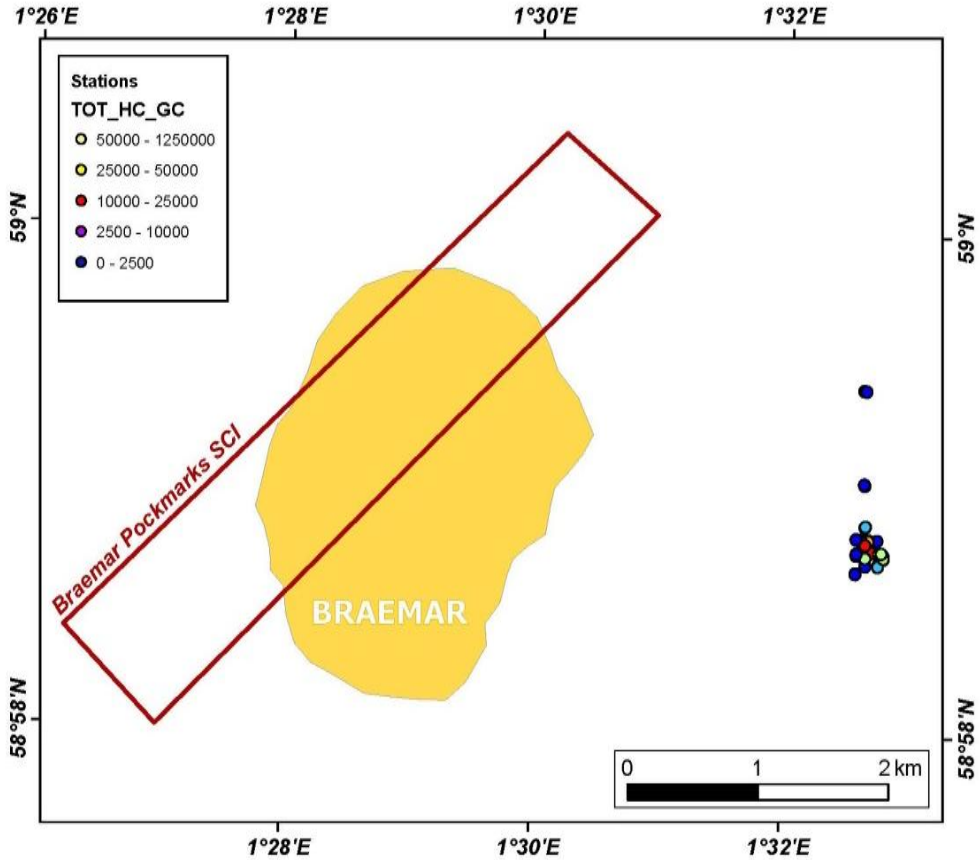

Figure 27. Spatial relationship between the Braemar Pockmarks SCI boundary and the seabed samples collected in the vicinity of the exploration well 16/3d-14.

Exploration well was spudded 4/4/96 and completed 2/6/96. The light yellow shading shows the Braemar Field. The sample points are colour coded according to the concentrations (in µg/g) of hydrocarbon in the sediments (determined by gas chromatography: TOT_HC_GC). Data extracted from the UK Benthos dataset.

The data on the UK benthos database includes the results from two surveys dated July 1996 and May 1997, both taken after the completion and abandonment of well 16/3d_14 on 2nd June 1996. The first survey shows elevated values for hydrocarbons (assumed to be attributable to the drilling of the well) of up to 40,000 µg/g (Figure 28). The second survey has a greater number of samples showing elevated concentrations of hydrocarbons, up to 110,000 µg/g (Figure 28). This increase in concentrations is not understood, but the combined data suggests that background levels exist 500 m from the well. Therefore it is reasonable to consider 500 m as a limiting extent for disturbed sediment to be transported on the seafloor in the vicinity of Braemar SCI.

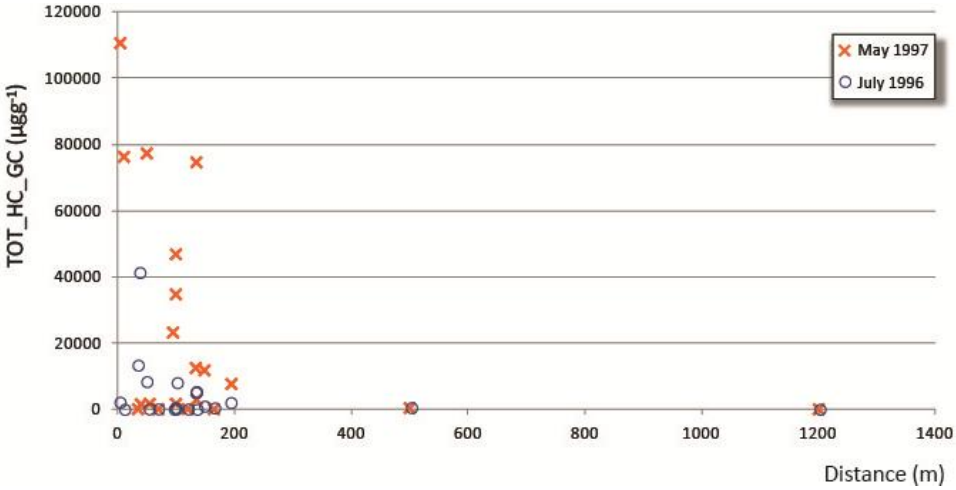

Figure 28. The concentrations of hydrocarbon in the sediments versus distance from the sample station to the exploration well 16/3d_14, for the two surveys extracted from the UK Benthos dataset.

6.2. Fishing Activity

It is generally accepted that the principal source of human physical disturbance of the seabed and seabed features is bottom trawl fishing (Hall-Spencer *et al.*, 2002). It is a major cause of concern with regard to the conservation of shelf and slope habitats and species (Gage *et al.*, 2005). Direct, immediate effects include scraping and ploughing of the substrate, sediment resuspension and destruction of benthos. The magnitude of the effect depends on the type of gear employed, the depth of penetration of the gear into the sediment, the water depth, the nature of the substrate (mud, sand, pebbles, or boulders), the kind of benthic communities being impacted (*i.e*. epibenthic *vs*. infauna), the frequency with which the area is fished, the weight of the gear on the seabed, the towing speed, the strength of the tides and currents, and the time of year. The long-term effects of bottom fishing disturbance is less well understood due to the complex nature of the changes and the lack of pre-impact or control data (Bradshaw *et al.*, 2002).

The parts of a trawl that leave the most distinctive marks are the otter boards. Single otter-board tracks range in width from approximately 0.2 to 2 m and their depths can vary from 3 to 30 cm deep (Krost *et al.,* 1990). Sediment type is one of the more important factors. In sandy sediment, there is low penetration of the otter boards due to high mechanical resistance of the sediment and the mobility of sand may lead to relatively rapid restoration, depending on waves and currents. Therefore, on sand-dominated seafloors the tracks are short-lived, whereas on muddy bottoms the tracks will be deeper and will last longer (Krost *et al.*, 1990).

The particle size analysis (PSA) of the samples recovered during the JNCC CEND19x/12 cruise from outside the pockmarks, show that the seabed in these area is mainly comprised of mud and sandy mud. These results are similar to BGS samples from the wider area (Table 2). In such soft sediments, lineations recognised on both side-scan sonar and multibeam backscatter data are interpreted as fishing trawl tracks. As there are no bedforms indicative of sediment migration it is possible that these linear features are the cumulative record of several decades of fishing activity. The position of the side-scan sonar data is not accurate enough to show if new scars were created by fishing activity in recent years or if old ones have been obscured by later sedimentation. Additionally, any apparent weakening or disappearance of these seabed features could also result from differences related to the equipment used and the orientation of data acquisition.

Figure 29 shows one example of a side-scan sonar line where fishing trawl tracks can be recognised on the seabed. Three individual fainted white tracks are visible; these may have been caused by the otter boards (~120 m apart) from a single traverse of a net. Their orientation would suggest that the net itself, between the two otter boards, was dragged through the pockmark and any weights / wheels along the throat of the net may have disturbed the seafloor within the pockmark, while one of the otter boards was dragged crossed the southern edge of Pockmark 48.

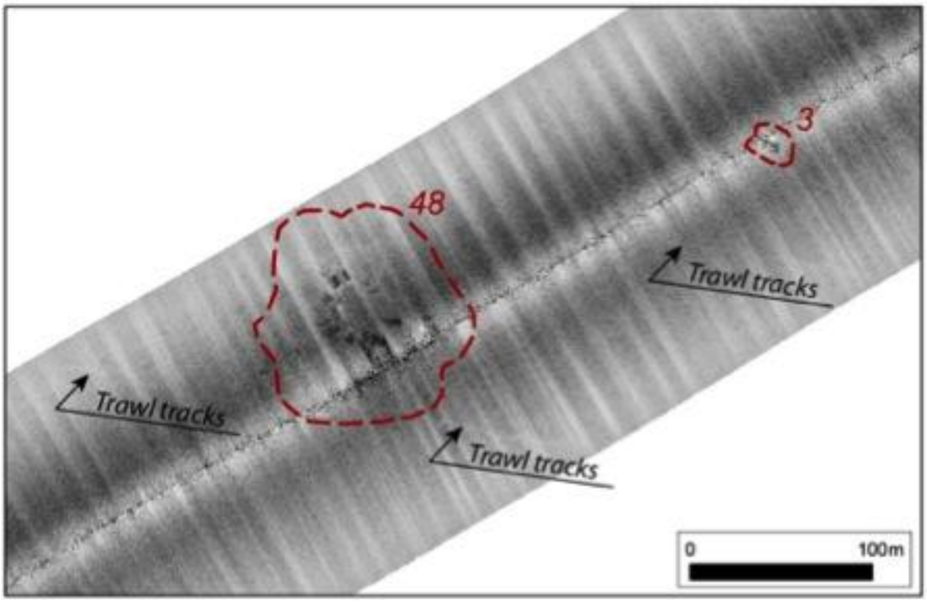

Figure 29. Detail view from one of the high frequency side-scan sonar line acquired during the CEND19x/12 cruise, showing three faint white trawl tracks at the seabed.

Trawling evidence is present throughout the surveyed area (Figure 30) and has been noted previously (Hartley, 2005), see Figure 16, although the marks noted in that earlier survey may have been anchor marks associated with rig emplacement for hydrocarbon drilling.

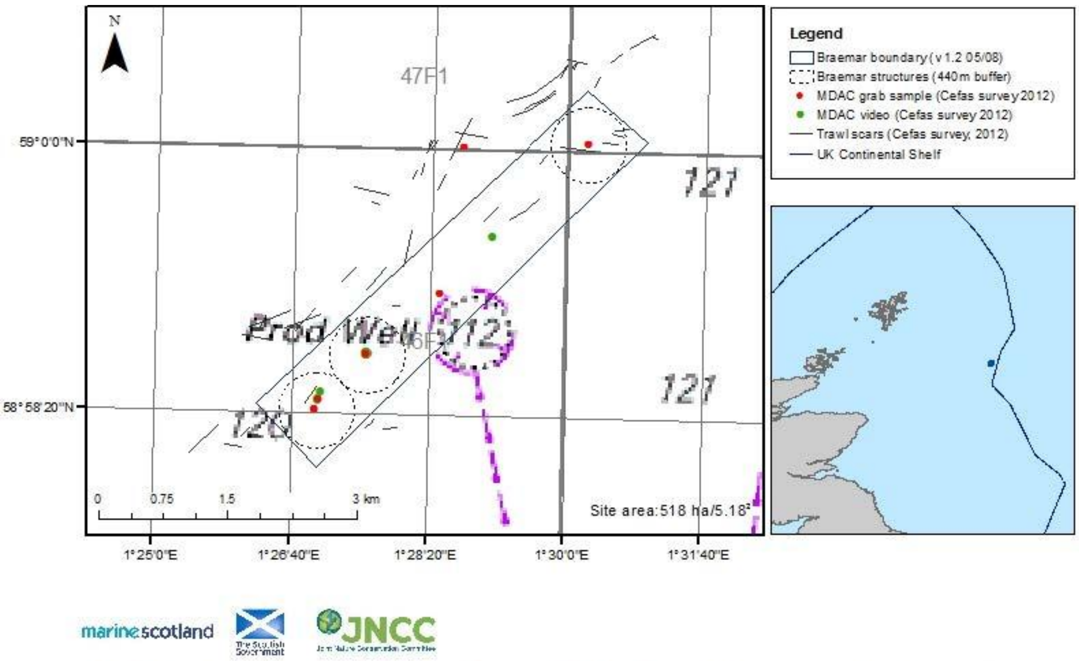

Map displayed in geographic coordinates WGS84. The exact limits of the UK Continental Shelf are set out in orders made under section 1(7) of the Continental Shelf Act 1964 (© Crown Copyright).Landmass Ordnance Survey © Crown Copyright and database right 2011. All rights reserved. Scotland (Adjacent waters) Updated by the Law of the Sea Division, United Kingdom Hydrographic Office October 2005. Fishing raster data ©DEFRA 2010. Fishing point data ©MS 2012.

Figure 30. Locations of trawl scars observed during JNCC survey in 2012

Figure taken from Braemar Pockmarks Site of Community Importance Fisheries Measures Proposal http://www.gov.scot/resource/0044/00442891.pdf

6.3. Debris

Discarded material from human activity (*e.g.* oil and gas or fishing) can be found on the seabed. Two of the seafloor images collected by JNCC (BRMR25_stn10_113 and BRMR42_S1_stn17_017) noted waste dropped to the seafloor.

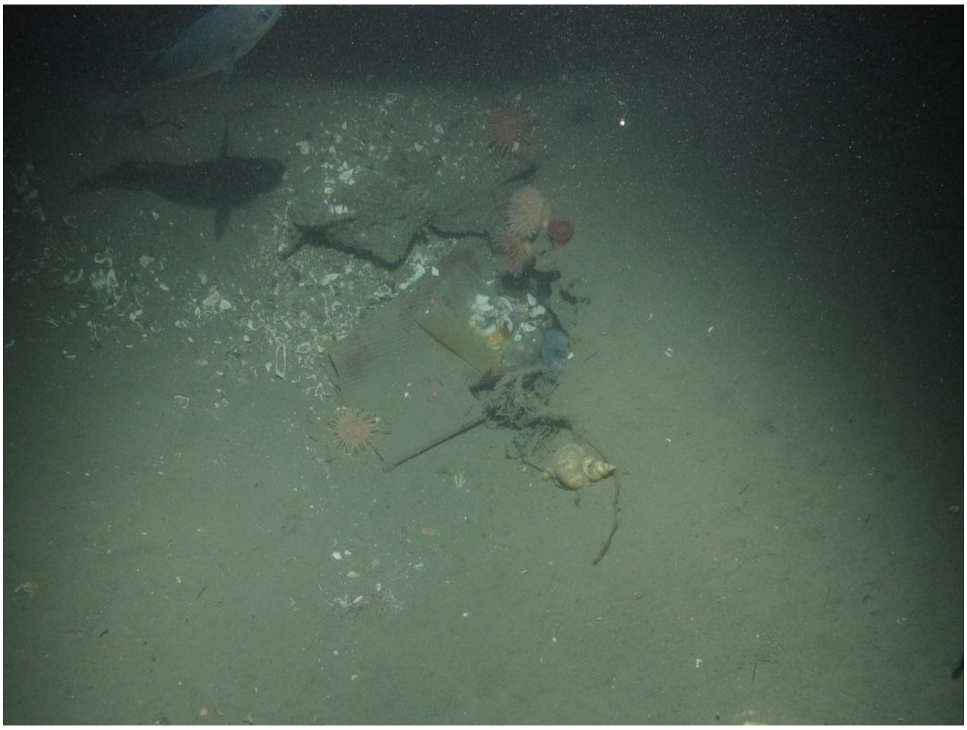

Figure 31. Waste dropped to the seafloor (matting and rope) observed on the JNCC cruise (CEND 19x/12) (Photo: BRMR25 Stn 10_113).

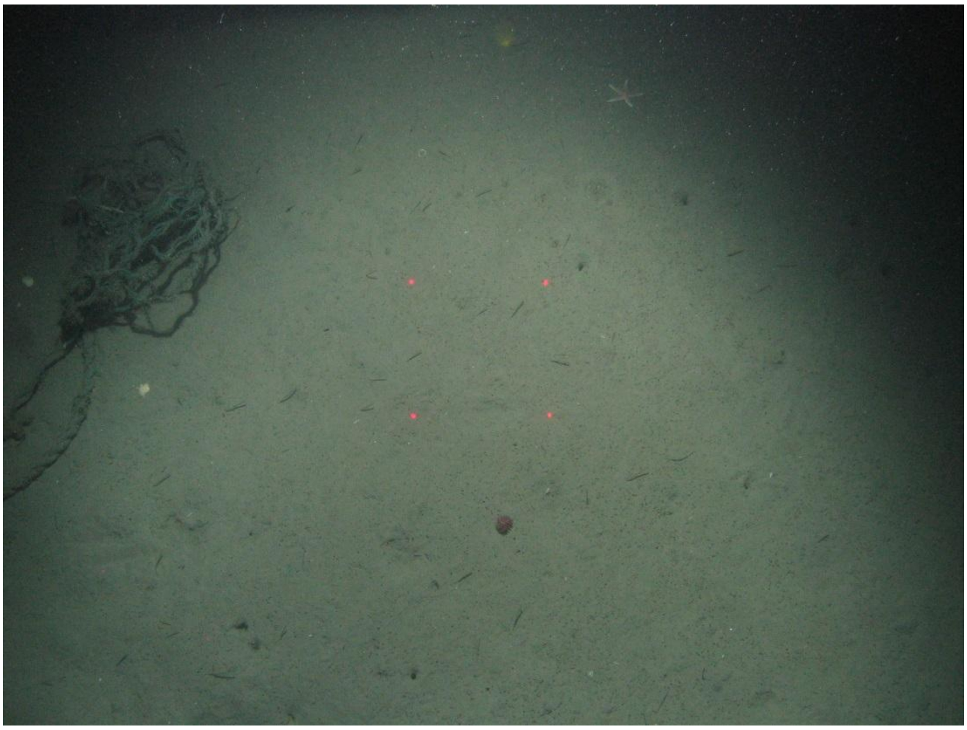

Figure 32. Waste dropped to the seafloor (rope) observed on the JNCC cruise (CEND 19x/12) (Photo: BRMR 42 Stn 17_017).

7. Comments

Choice of sampling sites:

Most of the 18 seabed samples collected from inside pockmarks were collected in areas affected by the lateral collapse of the pockmark's sidewall. Therefore, these samples may not be representative of the nature of the sediment found on the bottom of the pockmark. These samples present a high variability of sediment content that can be explained by their location within the slide deposits. Future sampling locations should be representative of the features of interest and should take account of the presence of collapsed material.

Direct evidence of seepage:

The Braemar Pockmarks SCI has not been as intensively surveyed in the past as the area covered by Scanner SCI area. The only evidence of gas escape recorded was the presence of water column targets on the side-scan sonar data uncorrected for slant-range. This suggests that the gas is emanating from pockmark 45 but where within the depression it is not possible to determine, nor if that can be related to the MDAC occurrences in that pockmark.

Geomorphological change:

The reasons for apparent change in pockmark geometry may be due to slope failure of the pockmark sidewall. Possible triggers include anthropogenic (*e.g.* fishing activity) as well as natural (*e.g.* pore pressure change associated with ground motion; seismic activity) or gas migration. Changes in geometry that include increases in depth may indicate removal of sediment during gas escape. Although some changes in pockmark geometry are indicated, differences in data acquisition and processing parameters prevent confident conclusions on the causes of pockmark changes.

Sedimentation:

The Braemar Pockmarks SCI is located in an area of negligible sedimentation since the early Holocene and therefore modern changes in individual pockmarks are likely to be due to processes associated with the pockmark or anthropogenic activities. They are not due to regional sediment deposition.

Limits of the SCI

Almost half the pockmarks mapped were found outside the present SCI area. These pockmarks are: 4, 5, 7, 9, 10, 11, 12, 13, 15, 17, 18, 22, 23, 24, 25, 26, 34, 36, 43, 44, 47 and 50. A total of 13 of the pockmarks mapped out of the Braemar Pockmarks SCI show areas of significant high backscatter that have been correlated to seabed exposures of MDAC. These pockmarks are 10, 12, 15, 17, 18, 24, 25, 26, 34, 36, 43, 44 and 50.

The wider regional picture shown in Figure 4 shows that pockmarks also exist outwith the area of the JNCC survey. This includes many in the seabed channel located just south of the Braemar Pockmarks SCI. There are more pockmarks on the higher seabed south of the channel. Other pipeline surveys close to Braemar Pockmarks SCI have noted MDAC on the floor of some of these pockmarks. It may be worth considering if the boundaries of the Braemar Pockmarks SCI include all the significant pockmarks with MDAC in the area.

Future surveys

In the space of the six years between the BP and the JNCC surveys, it appears that morphologic changes occurred on the seabed, probably due to slope instability and pockmark development. However, these observations are affected by a high level of uncertainty resulting from the different survey resolutions, positioning issues, and dataset artefacts. It would be relevant to conduct a third survey to minimize these uncertainties, preferentially using data acquisition and processing parameters equivalent to those used during the JNCC survey, in order to assess the level of gas escape activity. This survey should be conducted in approximately 5 years' time to preserve the same time lapse between the studies.

Future surveys may wish to include additional sampling to assess the leakage of gas such as chemical analysis of the water column and sediment porewaters. Chemical analysis of cores can show the location of oxidation and reduction fronts and where MDAC may form.

High-resolution seismic profiles may be able to distinguish whether slope failure within the pockmarks occurs as single or multiple events. However this would probably require a deep-towed seismic system to achieve the decimetre resolution needed.

Future processing of multibeam data should include examination of the water column to map bubble movement above the seabed. This has been done at the blow-out crater 22/4b (Schneider von Deimling *et al*., 2007), however the size of bubbles and their abundance at Braemar may be too small to be detected.

To establish whether or not there is a link between the gas leaking within the Braemar pockmarks and the gas reservoir at depth, and hence whether gas production from the Braemar reservoir will influence gas flow at the seabed, chemical analysis of the gas currently being released will be needed to assess its origin. It may be biogenic or petrogenic. Some information on the formation of MDAC can be obtained from chemical analysis of MDAC samples (Milodowski and Sloane, 2013). All of the aragonite and magnesium calcite cements display highly depleted 13C composition, with $\delta_{13}C_{PDB}$ values between -41 to -55 ‰, whereas the dolomite cements are -33.0 and -18.0 $‰_{PDB}$. These values are strongly indicative of carbonate cements precipitated as a result of methane oxidation, and are characteristic of MDAC deposits described previously from other areas (Milodowski and Sloane, 2013). The $\delta_{18}O$ analyses suggest that cementation occurred at two distinct times; once under cool to cold conditions, possibly during the Late Glacial, when high-magnesium calcite was precipitated and a second stage when aragonite was precipitated in conditions comparable to today (Milodowski and Sloane, 2013). It should be borne in mind that gas composition can be modified by microbes within sediments between deep reservoirs and the seabed and therefore very difficult to confirm whether the source of the methane is thermogenic or biogenic.

8. Conclusions

A total of 49 pockmarks were identified, mapped and characterised during this study. Of the mapped pockmarks, 27 are within the Braemar Pockmarks SCI boundary, 21 are less than 1 km away from the SCI limits and only one, pockmark 26, is situated more than 1 km.

The water depths over which pockmarks are found varies from 121.54 to 126.28, but only 9 of the mapped pockmarks are found in water deeper than 123.5 m. Most of the pockmarks are small to medium sized (330 to 11,000 m^2 in area); however one pockmark is considerably larger (with over 27,000 m^2). In total, more than 211,000 m^2 of the seabed were disrupted by these gas escape features. The majority of the pockmarks have a relief of between 1 m and 3 m; only 6 pockmarks of relief >3 m. These pockmarks have dimensions comparable to those found in other parts of the Witch Ground Basin.

Although they have comparable dimensions to pockmarks in the Witch Ground Basin, the pockmarks in Braemar Pockmarks SCI area tend to have rather irregular geometries, rarely presenting the typical circular or elliptical pockmark shape in plan-view and often presenting ‘W’-shaped or irregular profiles instead of the more typical ‘V’-shaped or ‘U’-shaped profiles seen in the Witch Ground Basin. Their geometry can be due to two main reasons: *1)* Multiple vents, and *2)* sidewall slope failure. In fact, nearly a quarter of the mapped pockmarks have evidence of slope failure. Slope instability is only observed in pockmarks with maximum slopes of more than 10°. Evidence suggests that one of these events occurred in the 6 year between the two surveys (Pockmark 32). The cause of slope failure is unknown, but may be either anthropogenic or natural.

In some cases the material mobilised by slope failure covers only a small area of the flat bottom of the pockmark, however in some pockmarks more than half of the bottom is occupied with collapsed material. Pockmark 48 shows one of the most marked cases of infilling by slope failure, with more than 65% of its central area filled with remobilised material which is more than half a meter thick. Features, such as MDAC, which may have been present at the seabed will have been buried.

Water column targets, taken as evidence of present day gas escape, were detected during the cruise CEND19x/12. This was observed in side-scan sonar data, uncorrected for slant-range, near pockmark 45. The presence of MDAC at seabed, an indirect evidence of seepage, was also found in the study area. MDAC was found in a total of 11 samples, recovered from six individual pockmarks (35, 38, 40, 48, 49 and 50) (Milodowski and Sloane, 2013). Based on the interpretation of both side-scan and multibeam backscatter and the recurrent presence of patches of high backscatter (that have been correlated to seabed exposures of authigenic carbonates), it is believed that other pockmarks in the study area may have MDAC at or near seabed. More than two thirds of the pockmarks show patches of high backscatter within the multibeam backscatter dataset, in some cases covering a significant part of the pockmark’s total area.

Several environmental effects of seepage are observed at the Braemar Pockmarks SCI: *1)* changes in the seafloor topography, *2)* changes in the physical composition of the seafloor (*i.e.*, sedimentological and mineralogical), *3)* development of hard substrates. Additionally, it can also be assumed that there may be: *1)* changes in the chemical composition of the seafloor, and *2)* changes in species composition.

The main potential sources of human physical disturbance to the seabed are related to oil and gas exploration and exploitation, or fishing activity. Evidence of both these activities is present in the Braemar Pockmarks SCI. There is a depression (of dimensions similar to the smaller mapped pockmarks) created by the drilling of the 16/03c-12 well, and several trawl scars recognized on both side-scan sonar and MBES backscatter. The latter activity (as well as E&P anchor handling operations) could modify the shape of existing pockmarks but there is no conclusive evidence that human activity has triggered slope failure, potentially leading to the burial of MDAC, and other features associated with gas seepage.

The results show that the Braemar Pockmarks SCI area is a location of active gas seepage, as evidenced by multiple indicators including exposed blocks of MDAC, bacterial mats and gas bubbles in the water column. It is suggested that the wider area should be monitored regularly to check if the features of interest are being compromised by natural or anthropogenic processes and to assess if the limits of the protected area are the most appropriate.

Appendix 1 Scope of work

The desk study will include the following for pockmarks within both Scanner and Braemar SCIs, although the Scanner and Scotia complex within Scanner SCI should be prioritised initially:

1. **Review the data collected from the 2012 JNCC** survey and specifically, **compare the multibeam and side-scan with similar from 2001** (SEA2) and other surveys, especially for morphological change across both sites. Note that no multibeam backscatter is available from the 2001 SEA2 data. Within Scanner Pockmark SCI, this should include the small pockmarks around the active site as well noting changes in the main pockmark features.
2. Compile a record of **observations indicative of gas seepage** within Scanner Pockmark SCI site boundary and Braemar Pockmarks SCI site boundary from the various surveys that have been run over the site.
3. Compile a record of **observations of methane derived authigenic carbonate (MDAC)** from the various surveys that have targeted the sites over time (including pre-submission) noting locations where this information is available within the two sites.
4. Examine and review **written records from previous JAGO submersible dive** (plus any ROV surveys from historic SEA/Government and industry surveys) and ascertain area of coverage – Within the two sites, **compare with coverage of drop down camera tows from JNCC 2012 survey**.
5. Examine and report on evidence for **anthropogenic causes of sedimentation**, including how trawlmarks have changed between 2001 and 2012. How many have disappeared, reflecting extent of active resedimentation? Examine the environmental monitoring of exploration wells near the active pockmarks within the two sites.
6. Provide details of **^{14}C datings in Witch Ground Basin** to give sedimentation rates outwith pockmarks, but which could be applied within the two sites (noting differences in PSA results between both sites) to understand natural sedimentation rates
7. Examine and report on zones of influence from historic work looking at **hydrocarbon wells/drill cuttings**. Look to apply this to grain sizes present within Scanner/Braemar area to provide estimates of a zone of influence from oil and gas exploration and production.

Note: Point 4 of scope of work presented above is not applicable to the Braemar Pockmarks SCI.

Appendix 2 Pockmarks Summary

Table 5. Pockmark characteristics inferred from the interpretation of the JNCC multibeam dataset.

ID	Lateral Collapse	Multiple Venting points	High Backscatter	In / Out of SCI
1	N		Y	In
3	N			In
4	N			Out
5	N			Out
6	N			In
7	N			Out
8	N			In
9	N			Out
10	N		Y	Out
11	n			Out
12	N		Y	Out
13	N			Out
14	N		Y	In
15	n	Y	Y	Out
16	minor		Y	In
17	N		Y	Out
18	N		Y	Out
19	N		Y	In
20	N	Y		In
21	N	y	Y	In
22	N			Out
23	N			Out
24	N		Y	Out
25	N	Y	Y	Out
26	N		Y	Out
27	Y		Y	In
28	n		Y	In
29	N		Y	In
30	N	y?	Y	In
31	N		y?	In
32	Y		Y	In
33	n		Y	In
34	N	Y	Y	Out
35	Y		Y	In
36	N		Y	Out
37	Y		Y	In
38	Y			In
39	N	y?	Y	In
40	Y		Y	In
41	N	Y	Y	In
42	N	Y	Y	In
43	Y		Y	Out
44	Y?		Y	Out
45	N	Y	Y	In
46	Y?		Y	In
47	N			Out
48	Y		Y	In
49	Y		Y	In
50	Y		Y	Out

Appendix 3 A review of pockmarks displaying greatest differences between the BP and JNCC datasets

Section 3.4 compared the bathymetric datasets created from the 2006 multibeam survey commissioned by BP with that derived from the multibeam survey collected by JNCC in 2012. Differences were noted in the depths of individual pockmarks (Figure 13) and in the location of the deepest point within individual pockmark (Figure 14). Small differences probably reflect differences in the algorithms used in multibeam surveys. If there are n the ual pockmark (Figure ssioned by BP with that derived from the s considered most appropriate to examine those pockmarks with greatest change in pockmark depth and/or change in position of the deepest point within a pockmark. Differences of more than 50 cm were observed in the depth of ten pockmarks (9, 10, 15, 18, 20, 26, 32, 41, 45 and 48). Differences of more than 12.5 m in the location of the deepest points within a pockmark were noted in six pockmarks (9, 17, 30, 34, 43 and 48).

Due to their dimensions and marked differences between datasets, it was not possible to assess the nature of the differences noticed within pockmarks 9, 10 and 15.

Pockmark 17 appears to show evidence of deepening during the time between the two surveys, particularly on the eastern side.

Pockmark 18 shows a wider, ‘W’-shaped, profile in the JNCC dataset than on the BP dataset, where it is shallower and ‘V’-shaped.

The changes in pockmark 20 could not be precisely resolved.

Pockmark 26 appears to have become ~50 cm deeper and some profiles extracted from the JNCC dataset present a ‘V’ shape more marked in the central section than in their equivalent for the BP dataset.

No significant changes were noticed between the ‘U’-shapes profiles extracted from pockmark 30. The deepest point appears to have migrated 12.5 m from one survey to the other; slightly further than would be attributed to the lateral shift between the two datasets. However, this pockmark is characterised by a marked U-shaped profile (broad flat bottom), which can lead to a larger uncertainty in the identification of its deepest point, therefore this apparent migration of the deepest point is not considered to require further investigation.

Pockmark 32 exhibits a deepening of more than 50 cm between the 2 surveys, and the pockmark profiles evolved from a standard ‘V’ shape in the BP dataset to a ‘W’ or asymmetric ‘V’ shape in the JNCC dataset. This increase in complexity is believed to be the result of slumping on the south-eastern sidewall. This suggests that slope failure occurred during the six years between the two surveys.

Pockmark 41 is composed of two deeper areas 35 meters apart resulting from multiple venting points (or the amalgamation of two adjacent pockmarks). Deepening and a widening of the southern depression between the two surveys is suggested. No significant changes were observed in the northern depression.

Pockmark 43 has a flat bottom 40 meters wide, which makes the determination of its deepest point extremely sensitive to vertical shifts on the datasets. Therefore, the apparent discrepancy of almost 26 m is believed to be an artefact of the data processing.

Pockmark 45 has multiple deep points. There is an apparent deepening of the deepest. However, due to the complex pockmark geometry and differences between the surveys, it is not possible to characterize other morphologic changes associated with this pockmark.

The depth estimates for pockmark 48 suggest significant (0.93 m) deepening between the two surveys. However, further investigation shows that part of the pockmark was not integrated in the pockmark depth estimation for the BP dataset. Extracting the profiles revised the estimated deepening to approximately 0.25 m. Most of the bottom of pockmark 48 appears to be infilled by slump material from the eastern sidewall. This material was already present when the BP dataset was acquired, however some changes to the geometry may have occurred between the acquisition of the two datasets.

Appendix 4 UK Benthos data from well 16/3d-14

UK Benthos is a database of offshore environmental benthic surveys since 1975, in the UK sector of the North Sea. These data were brought together by oil companies that were members of the United Kingdom Offshore Operators Association (now Oil & Gas UK). The database is accessible via the Internet, see:

http://www.oilandgasuk.co.uk/knowledgecentre/uk_benthos_database.cfm.

The table below is an extract of this dataset with information referring to well 16/3d-14 (58° 58.6533'N; 01° 32.6640'E), used as an analogue for sediment movement near the Braemar Pockmarks SCI.

Table 6. Data extracted from the UK Benthos dataset for well 16/3d-14 (58° 58.6533'N, 01° 32.6640'E).

Site (sample site unique code), year and month of sampling, station location in UTM, distance from the well to the site in meters, the sediment median grain size in Phi units (MDO), the sediment silt/clay content (Silt/Clay), and the hydrocarbon content determined by gas chromatography in µg/g (TOT_HC_GC).

Site	Year	Month	UTM E	UTM N	Distance	MDO	Silt/Clay	TOT_HC_GC
WW396C1	1996	JUL	416321	6538611	4	2.9	43.71	-
WW396C2	1996	JUL	416321	6538604	11	4.2	53.51	-
WW396C3	1996	JUL	416316	6538650	36	3.58	23.4	-
WW396C4	1996	JUL	416341	6538713	101	3.27	14.06	-
WW396C5	1996	JUL	416296	6538713	101	3.33	13.95	163
WW396C6	1996	JUL	416315	6538811	197	3.31	15.85	-
WW396C7	1996	JUL	416264	6538608	54	3.35	15.19	150
WW396C8	1996	JUL	416368	6538614	50	3.25	15.78	8373
WW396C9	1996	JUL	416320	6538517	97	3.33	15.8	42.8
WW396C10	1996	JUL	416414	6538705	136	3.36	16.02	38.4
WW396G1	1996	JUL	416320	6538610	4	3.75	24.08	2141
WW396G2	1996	JUL	416321	6538625	12	3.5	23.07	8.5
WW396G3	1996	JUL	416311	6538649	35	3.2	22.48	13336
WW396G4	1996	JUL	416343	6538709	99	3.13	15.21	510
WW396G6	1996	JUL	416320	6538808	194	2.97	11.26	2052
WW396G11	1996	JUL	416320	6539117	503	3.1	15.49	522
WW396G12	1996	JUL	416321	6539816	1202	3.01	14.68	7.7
WW396G13	1996	JUL	416250	6538717	121	3.06	14.37	99
WW396G14	1996	JUL	416250	6538598	70	3.12	15.67	145
WW396G15	1996	JUL	416244	6538466	166	3.01	12.11	432
WW396G16	1996	JUL	416291	6538589	38	3.49	24.32	41338

WW396G17	1996	JUL	416420	6538615	102	3.18	19.04	8061
WW396G18	1996	JUL	416415	6538521	135	3.16	15.83	5376
WW396G19	1996	JUL	416461	6538570	149	3.04	13.28	972
WW396G20	1996	JUL	416451	6538603	134	3.12	17.07	5060
WW397C1	1997	MAY	416325	6538608	5	5.8	69	-
WW397C2	1997	MAY	416321	6538614	11	5.9	72.3	-
WW397C3	1997	MAY	416312	6538653	35	3.6	23.1	-
WW397C4	1997	MAY	416349	6538720	100	3.8	25.6	-
WW397C6	1997	MAY	416319	6538815	195	3.8	74.5	-
WW397G1	1997	MAY	416315	6538607	5	6.5	87.2	110570
WW397G2	1997	MAY	416317	6538624	11	5.7	76.6	76221
WW397G3	1997	MAY	416317	6538648	35	4.6	73.2	2.3
WW397G4	1997	MAY	416343	6538704	100	4.8	50.4	46793
WW397G5	1997	MAY	416292	6538706	100	3.6	29.1	1634
WW397G6	1997	MAY	416324	6538812	195	3.9	29.9	7628
WW397G7	1997	MAY	416263	6538617	55	3.9	30.6	1617
WW397G8	1997	MAY	416376	6538617	50	6.1	78	77265
WW397G9	1997	MAY	416320	6538577	95	5.1	46.9	23162
WW397G10	1997	MAY	416322	6538676	135	5.5	56.3	74568
WW397G11	1997	MAY	416318	6539122	500	3.8	26.9	333
WW397G12	1997	MAY	416338	6539814	1200	3.7	21.6	0.42
WW397G13	1997	MAY	416250	6538720	120	3.8	28.1	49.7
WW397G14	1997	MAY	416252	6538610	70	3.8	26.2	14.3
WW397G15	1997	MAY	416243	6538463	165	3.8	25.4	8.8
WW397G16	1997	MAY	416461	6538591	40	4	37.9	1479
WW397G17	1997	MAY	416425	6538612	100	4	45.2	34695
WW397G18	1997	MAY	416417	6538515	135	3.9	30.4	2859
WW397G19	1997	MAY	416461	6538572	149	4	42.9	11750
WW397G20	1997	MAY	416446	6538609	134	3.9	35.9	12473

Appendix 5 Seismic sections location map

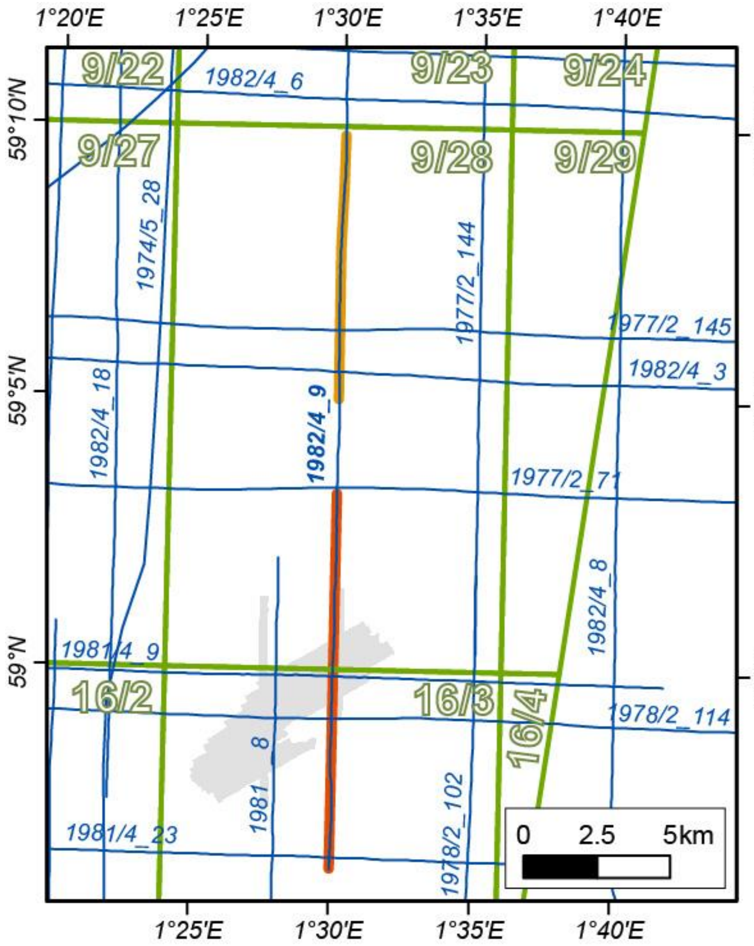

Figure 33. BGS geophysical survey lines within the vicinity of Braemar SCI showing the location of Figure 19 (red highlight) and Figure 23 (orange highlight).

Glossary

Authigenic	Formed *in situ*
BGS	British Geological Survey
BODC	British Oceanographic Data Centre
DDM	Digital depth model
DECC	Department of Energy and Climate Change
Holocene	The geological epoch beginning at the end of the last ice age, spanning the last 10,000 years. Together with the preceding Pleistocene epoch forms the Quaternary period.
Late Glacial	Period of time following the last glacial maximum whilst ice sheets waned but subject to extensive periglacial and paraglacial conditions prior to the onset of temperate conditions of the Holocene.
JNCC	Joint Nature Conservancy Committee
MBES	Multibeam Echo Sounder
MDAC	Methane-Derived Authigenic Carbonate
Pleistocene	The geological epoch from 2.5 million to 10,000 years ago. This period of time was characterized by frequent climatic changes from ice ages to interglacial conditions.
PSA	Particle Size Analysis
SCI	Site of Community Importance
SSS	Side-scan Sonar
TWT	Two-way-Time
ROV	Remotely-Operated Underwater Vehicle
UKCS	United Kingdom Continental Shelf
WGF	Witch Ground Formation, a seismostratigraphic geological unit thought to be of Late Glacial to Holocene age.

References

The British Geological Survey holds most of the references listed below, and copies may be obtained via the library service subject to copyright legislation (contact libuser@bgs.ac.uk for details). The library catalogue is available at: http://geolib.bgs.ac.uk.

Andrews, I.J., Long, D., Richards, P.C., Thomson, A.R., Brown, S., Chesher, J.A. and McCormac, M. 1990. United Kingdom offshore regional report: The Geology of the Moray Firth. London: HMSO for the British Geological Survey. 93pp.

Berry, J.A., and Wells P.G. 2004. Integrated fate modeling for exposure assessment of produced water on the Sable Island Bank (Scotian Shelf, Canada). *Environmental toxicology and chemistry*, 23, 2483-2493.

Boetius, A., Ravenschlag, K., Schubert, C.J., Rickert, D., Widdel, F., Gieseke, A., Amann, R., Jørgensen, B.B., Witte, U. and Pfannkuche, O. 2000. A Marine Microbial Consortium Apparently Mediating Anaerobic Oxidation of Methane. *Nature*, 407, 623-626.

Bradshaw C., Veale L.O. and Brand A.R. 2002. The role of scallop-dredge disturbance in long-term changes in Irish Sea benthic communities: a re-analysis of an historical dataset. *Journal of Sea Research,* 47, 161-184.

Bradwell, T., Stoker, M., Golledge, N., Wilson, C., Merritt, J., Long, D., Everest, J., Hestvik, O.B., Stevenson, A., Hubbard, A., Finlayson, A., Mathers, H. 2008. The northern sector of the Last British Ice Sheet: maximum extent and demise. Earth Science Reviews, 88, 207-226.

British Geological Survey. 1986. Bressay Bank, Sheet 59° N-00°, Quaternary Geology. 1:250000. (Keyworth, Nottingham: British Geological Survey).

British Geological Survey. 1986. Fladen, Sheet 58° N-00°, Sea Bed Sediments. 1:250000. (Keyworth, Nottingham: British Geological Survey).

British Geological Survey. 1987. Bressay Bank, Sheet 59° N-00°, Sea Bed Sediments. 1:250000. (Keyworth, Nottingham: British Geological Survey).

British Geological Survey. 1988. Fladen, Sheet 58° N-00°, Quaternary Geology. 1:250000. (Keyworth, Nottingham: British Geological Survey).

CEFAS and JNCC, 2013. Braemar CSAC, Scanner CSAC and Turbot Bank SMPA Search Location Survey Report. 132pp.

Dando, P.R. 2010. Biological communities at marine shallow-water vent and seep sites. In: Kiel, S. (Ed.), The vent and seep biota – from microbes to ecosystems. *Topics in Geomicrobiology*, 33, 333-378.

Dando, P. R. Austen, M.C. Burke R.A. Jr, Kendall, M.A. Kennicutt, M.C. II Judd, A.G. Moore, D.C. O'Hara, S.C.M. Schmaljohann, R. Southward, A.J. 1991, Ecology of a North Sea pockmark with an active methane seep, *Marine Ecology Progress Series*, 70, 49-63.

DECC, 2013. Offshore Oil & Gas Licensing 27th Seaward Round Central North Sea Blocks 9/27, 15/20f, 15/24a, 15/25c, 16/2c, 16/16. Habitats Regulations Assessment Appropriate Assessment. 34 pp.

Elkins, S.R. 1977 Recent Sediments of the Northern North Sea: Factors Controlling Their Composition and Distribution (*MSc dissertation*, University of Minnesota).

Erlenkeuser, H. 1979. Environmental Effects on Radiocarbon in Coastal Marine Sediments. 453-469 *In*: Berger, R. and Suess, H.E. (Eds) *Radiocarbon Dating*, University of California Press.

Gafeira, J, Long, D and Diaz-Doce, D. 2012. Semi-Automated Characterisation of Seabed Pockmarks in the Central North Sea. *Near Surface Geophysics*, 10 (4), 303–314.

Gage, J.D., Roberts, J.M., Hartley, J.P. and Humphery, J.D. 2005. Potential impacts of deep-sea trawling on the benthic ecosystem along the northern European continental margin: a review. *In:* Barnes, P. W. & Thomas, J. P. Eds. Benthic habitats and the effects of fishing. *American Fisheries Society Symposium* 41: 503-517.

Hall-Spencer, J., Allain, V. and Fosså, J.H. 2002. Trawling Damage to Northeast Atlantic Ancient Coral Reefs. *Proceedings of the Royal Society of London*, B. 269, 507-511.

Hartley, J. P. 2005. Seabed Investigations of Pockmark Features in UKCS Block 16/3. Report to Joint Nature Conservation Committee. Aberdeenshire: Hartley Anderson Limited.

Hedges, R.E.M, Housley, R.A., Law, I.A., Perry, C. and Hendy, E. 1988. Radiocarbon Dates From The Oxford Ams System, Archaeometry Datelist 8, *Archaeometry* 30, 291305.

Holmes, R. 1977. Quaternary Deposits of the Central North Sea 5. The Quaternary Geology of the UK Sector of The North Sea, between 56° and 58° N. Report of the Institute of Geological Sciences, No. 77/14.

Hovland, M. and Sommerville, J. 1985. Characteristics of Two Natural Gas Seepages in the North Sea. *Marine and Petroleum Geology*, 2, 319-326.

Hovland, M. and Judd, A.G. 1988. *Seabed pockmarks and seepages impact on geology, biology and the marine environment*. Graham & Trotman, LondonHovland, M., Jensen, S. and Fichler, C. 2012. Methane and Minor Oil Macro-Seep Systems - Their Complexity and Environmental Significance. *Marine Geology*, 332–334, 163-173.

Hovland, M., Talbot, M.R., Qvale, H., Olaussen, S. and Aasberg, L. 1987. Methane-Related Carbonate Cements in Pockmarks of the North Sea. *Journal of Sedimentary Research*, 57, 881 – 892.

JNCC, 2012. Offshore Special Area of Conservation: Braemar Pockmarks. SAC Selection Assessment Document. Version 4.1 http://jncc.defra.gov.uk/PDF/BraemarPockmarks_SelectionAssessment_4.1.pdf

Johnson, H., Richards, P C., Long, D. and Graham, C C, 1993. United Kingdom Offshore Regional Report, The Geology of the Northern North Sea. British Geological Survey Regional Report.

Johnson, T.C. and Elkins, S.R. 1979. Holocene Deposits of The Northern North Sea: Evidence for Dynamic control of their mineral and chemical composition. *Geologie En Mijnbouw*, 58, 353-366.

Judd, A.G. 2001. Pockmarks in the UK Sector of the North Sea, Technical Report TR_002, Technical report produced for Strategic Environmental Assessment - SEA2, DTI.

Judd, A.G. and Hovland, M. 2007. *Seabed Fluid Flow. The Impact on geology, biology and the marine environment*. Cambridge University Press. 475 pp.

Judd, A.G., Long, D. and Sankey, M. 1994. Pockmark Formation and Activity, UK Block 15/25, North Sea. *Bulletin of the Geological Survey of Denmark*, 41, 34-49.

Krost, P., Bernhard, M., Werner, F. and Hukriede, W. 1990. Otter trawl tracks in Kiel Bay (Western Baltic) mapped by side-scan sonar. *Meeresforsch* 32, 344-353.

Long, D**.** 1991. The identification of features due to former permafrost in the North Sea. In: Forster, A., Culshaw, M.G., Cripps, J.C., Little, J.A. and Moon, C.F. (eds) *Quaternary Engineering Geology*, Geological Society of London, *Engineering Geology Special Publication*, No 7, 369-372.

Long, D. 1992. Devensian Late-Glacial Gas Escape in the Central North Sea. *Continental Shelf Research*. 12 (10), 10971110.

Long, D. and Morton, A.C. 1987. An Ash Fall within the Loch Lomond Stadial. *Journal of Quaternary Science*, 2, 97101.

Long, D., Bent, A., Harland, R., Gregory, D.M., Graham, D.K. and Morton, A.C. 1986. Late Quaternary Palaeontology, Sedimentology and Geochemistry of a Vibrocore from the Witch Ground Basin, Central North Sea. *Marine Geology*, 73, 109123.

Milodowski, A. E. and Sloane, H. 2013. Petrography and stable isotope study of methane-derived authigenic carbonates (MDAC) from the Braemar Pockmark Area, North Sea. *British Geological Survey Commissioned Report*, CR/13/078. 112pp.

Schneider von Deimling, J., Brockhoff, J. and Greinert, J. 2007 Flare imaging with multibeam systems: Data processing for bubble detection at seeps, *Geochemistry, Geophysics, Geosystems*, 8, Q06004, doi:10.1029/2007GC001577.

Stoker, M.S. and Long, D. 1984. A Relict Ice-Scoured Erosion Surface in the Central North Sea. *Marine Geology*, 61, 8593.

Stoker, M.S., Long, D. and Fyfe, J.A. 1985. A revised Quaternary Stratigraphy for the Central North Sea. British Geological Survey, Report No. 17/2.